CHAPTER 3

RESULTS

3.1) INVESTIGATION OF PROTEIN EXPRESSION IN COLD SHOCK AT DIFFERENT TEMPERATURES.

3.1.1 Growth Profiles of *B. stearothermophilus* TLS33 under Cold Shock

The downshift in temperature intends to know a transient metabolic adaptation for bacterial survival and its physiological activity. The bacterial cultures were incubated at 65°C for 24 h before temperature were subjected to 37°C and 25°C that are the normal bacterial growth temperature and room temperature, respectively. The bacteria growths were followed in several hours and the growth profile of these bacteria is shown in Figure 3.1. the mid-log phase at 24 hours (OD_{620}~0.5, T = 0 hours) of bacterial growth curve was chosen for cold shock experiment, in order to get enough number of cells that begin to synthesizing different proteins and others including primary and secondary metabolites that appear to make the cell more resistant to certain environmental conditions. After cold shock at 37°C and 25°C that nevertheless permit growth, the growth of this bacterium decreased immediately in the initial cold shock for 2 hours and slow down to equilibrium growth after 4 hours while the bacterium at 65°C continued its growth up to 8 hours (T = +8 hours). Although the bacteria after cold shock stress decreased their growths, but they were still alive that visualized under microscope and stable up to 8 hours in the cold with the optical density approximately 0.30-0.35. In addition, cell extracts after temperature downshifts from 65°C to 37°C and from 65°C to 25°C for 2 hour showed

no significant differences in total protein concentrations which were estimate 3.0 mg/ml. Therefore, the major difference in cold induced proteins was occurred at 2 h after downshift in temperature and also showed a significant cold shock response in protein expression and protein synthesis that related to bacterial adaptation in sporulation (71)

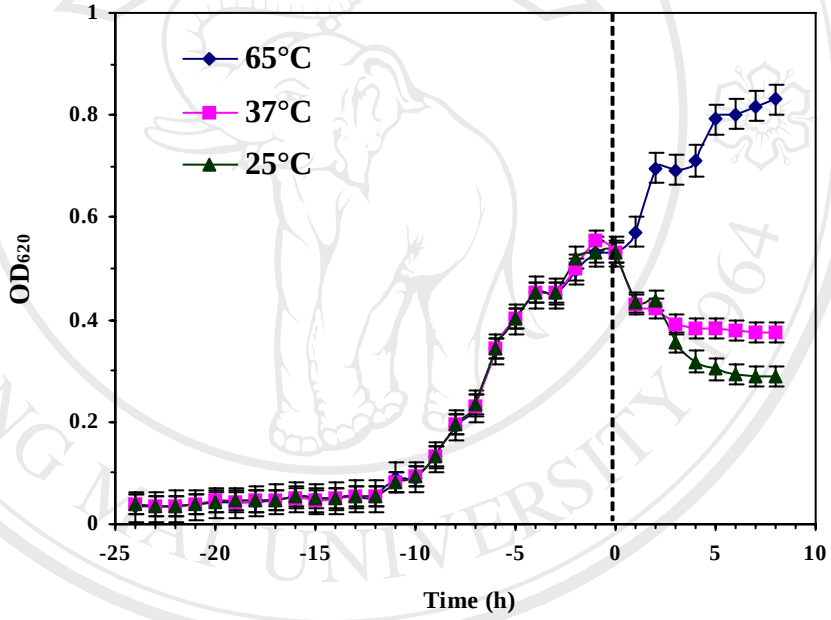

Figure 3.1 Growth profile of *B. stearothermophilus* TLS33 under cold shock stress at 37°C and 25°C for 2 h. Cold chock stress is induced at the 24 h-cultivation time of cell growth (T = 0 h, starting cold shock stress) until 8 h of induction (T = 8 h).

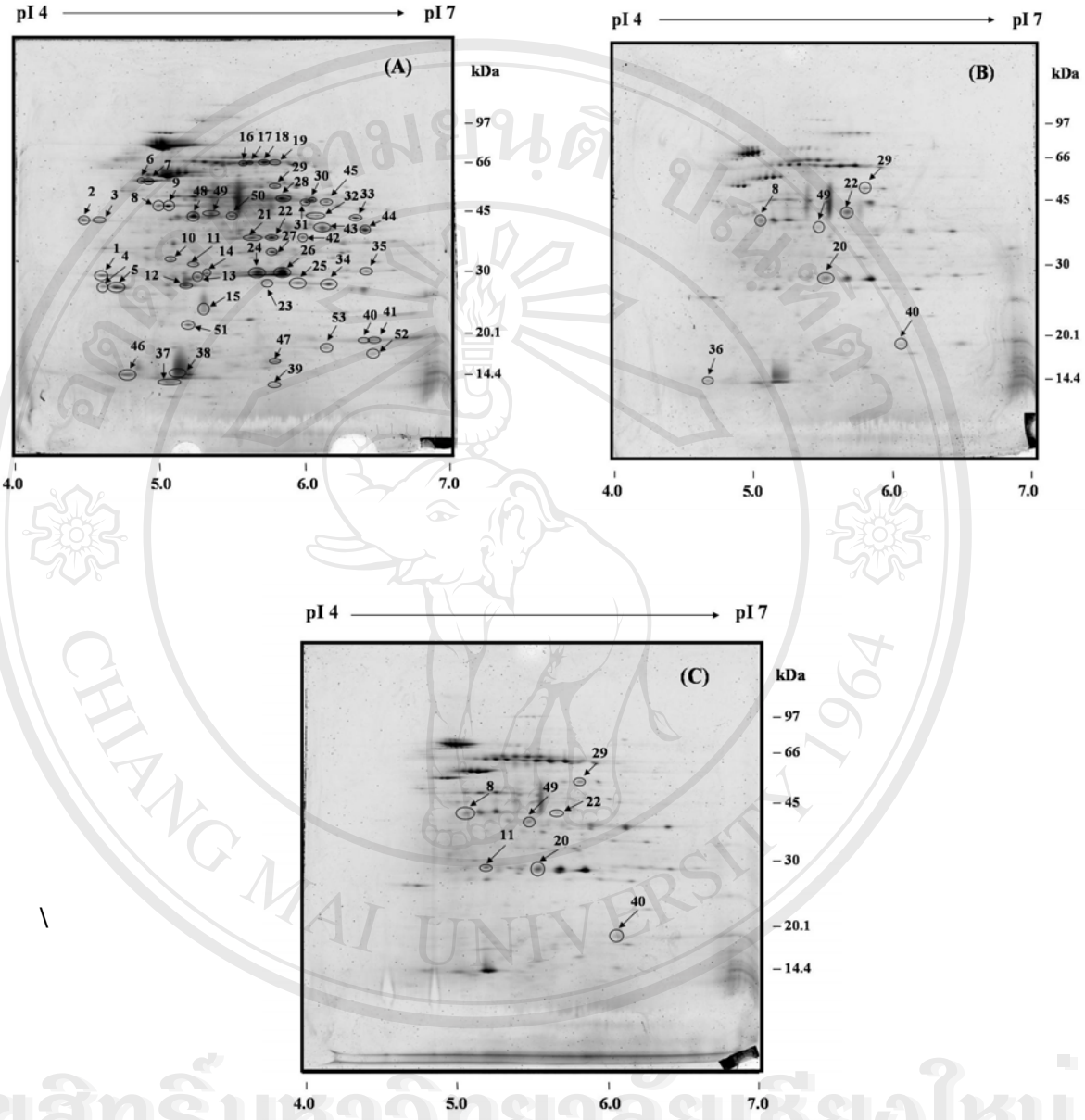

Figure 3.2 2-D gel patterns of cell extracts from *B. stearothermophillus* TLS33 under different temperatures (A, 65°C; B, 37°C; C, 25°C). The arrows show the spots of proteins which identified by MALDI-TOF mass spectrometry.

3.1.2 2 DE of cold shock stress at different temperatures

The downshift in temperature from 65°C to 37°C and 25°C after 2 hours showed a significant cold shock response in protein expression as analyzed by 2-D PAGE (Figure 3.2). Abundant proteins were expressed at 65°C that demonstrated on 2-D gels in a narrow pH range of 4-7 (Figure 3.2A) while fewer proteins were expressed at 37°C and 25°C, respectively (Figure 3.2B, 3.2C). Almost no proteins were observed in the pH ranges of 3-4 and 7-11 for all 3 experimental temperatures. Therefore, we focused to search for cold shock-induced proteins within a narrow pH range of 4-7. This is similar to other reports demonstrating that the number of cold-induced proteins identified in *B. subtilis* is much greater than those characterized for *E. coli* and the examinations carried out so far were restricted to a rather narrow *p*I 4-7 and MW range of 5-100 kDa (71-73).

Although, the protein distribution patterns in 2-D gels were similar in all temperatures but the image analysis software of ImageMaster 2D Elite was used for protein analysis and comparison of 2-D images. The total detected proteins on 2-D gels of the cell extracts at 65°C, 37°C and 25°C were 191, 116 and 115 proteins, respectively. Comparisons between cell extracts in different group temperatures (37°C and 65°C, 25°C and 65°C, and 37°C and 25°C) showed the matching proteins of 66, 57 and 75 spots with 34.55%, 29.84% and 64.65% matching, respectively. The differential protein expressions under cold shock stress showed the synthesis of proteins was suppressed in term of down-regulation and overexpressed in term of up-regulation. The pair-wise comparisons between cell extracts at different group temperatures (37°C and 65°C, 25°C and 65°C, and 37°C and 25°C) showed 44, 25 and 10 up-regulated proteins, respectively. While the numbers of down-regulated

proteins were 20, 29 and 12, respectively. The up- and down-regulations of expressed proteins were also used a linear scattering plot with y = 10x (up-regulation), y = x (equal) and y = 0.1x (down-regulation) (Figure 3: 3 A, B and C). Furthermore, we found that the synthesis of major intracellular proteins decreased following cold shock and 53 proteins showed the significantly changed between three temperatures whereas only 8 major cold-induced proteins had markedly changed under cold shock stress.

The 49 spots of proteins were expressed at the temperature of 65°C while 8 spots of proteins were significantly differential expressed under temperatures of 37°C and 25°C. The cold-induced proteins at both 37°C and 25°C were glucosyltransferase, an anti-sigma B (σ^B) factor (RsbT), Mrp protein homolog, dihydroorthase, hypothetical transcriptional regulator in the FeuA-SigW intergenic region, RibT protein, phosphoadenosine phosphosulfate reductase, and prespore specific transcriptional activator RsfA. However, the cold-induced proteins in 37°C and 25°C were different only 1 protein that was RibT protein and anti-σ^B factor (RsbT), respectively (Figure 3.4). In figure 3.4, these 8 cold induced proteins were classified into 3 group, i.e. 1) proteins expressed under low temperature at 37°C 2) Proteins expressed at 37°C only 3) The proteins expressed at 65°C and 25°C.

(A)

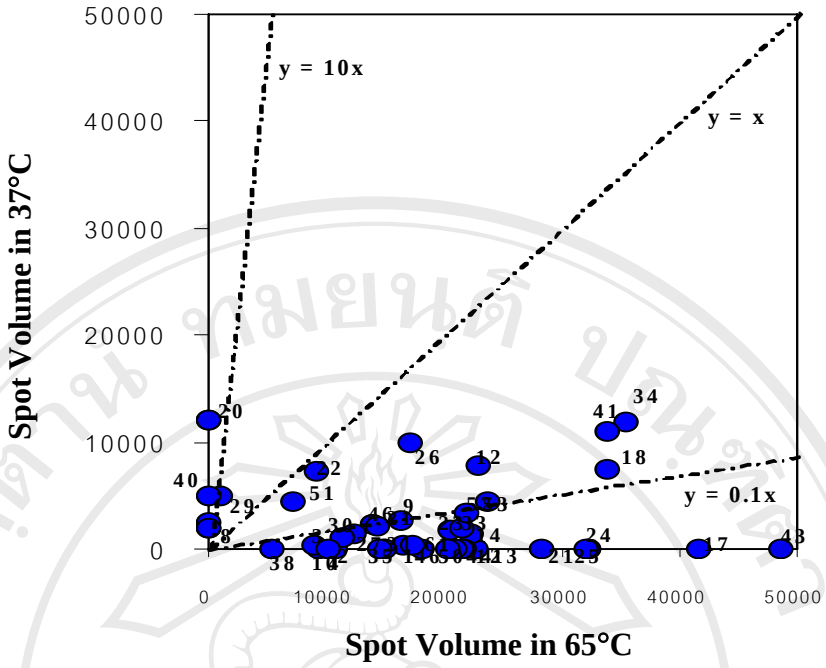

(B)

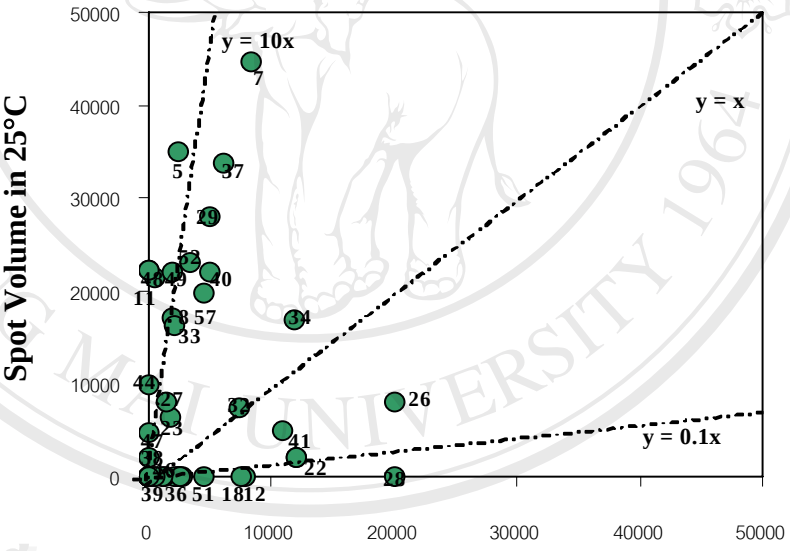

Figure 3.3 Up- and down-regulation of proteins from *B. stearothermophilus* TLS33 after temperature downshift from 65°C to 37°C and 25°C, demonstrating by ImageMaster 2D Elite software. A), comparison between the temperatures at 37°C and 65°C (B) comparison between the temperatures at 37°C and 25°C

(C)

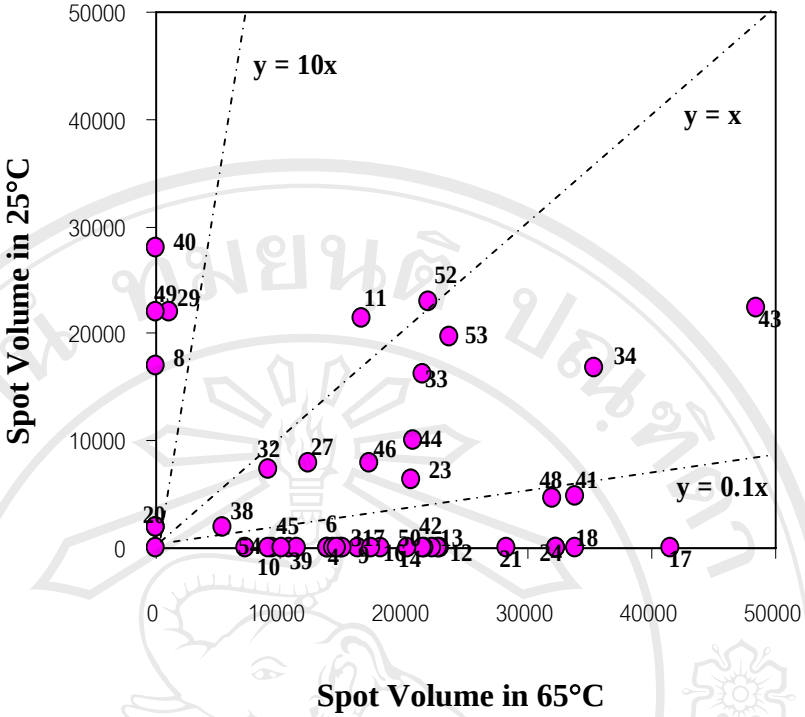

Figure 3.3 (continued) (C) comparisons between the temperatures at 65°C and 25°C

3.1.3 Protein Identification and Differential Protein Synthesis

The 53 spots of total proteins on 2-D gels from cell extracts in three temperatures were selectively identified by MALDI-TOF mass spectrometry and searched on SwissProt and NCBI non-redundant database with the MS-FIT and MASCOT software. In addition, SubtiList database (http://genolist.pasteur.fr/SubtiList) supplementing with EMBL/GenBank/DDBJ databases is used for identification of the cytosolic proteins including cold shock-induced proteins in *B. stearothermophilus* TLS33 as shown to be the identified proteins and genes including accession numbers, description and functional category (Table 3.1).

3.1.4 Cold Shock Effect on Signaling Pathways of *B. stearothermophilus* TLS33

Using the proteomic techniques and bioinformatics, the identified proteins were correlated back to the genome level and attempted to locate their gene loci. Eight differentiated cold shock-induced proteins were observed their function and found only six proteins encoded genes correlate to the signaling pathways of sporulation. The identified proteins encoded genes TagE, YbbB, RsfA, RsbT, MrpA and PyrC were related to the σ^F and σ^G factors on this 'Forespore' stage of the sporulation process (74).

Herein, the identified proteins in the following routes which lead in sporulation were interpreted by correlation the signaling protein in sporulation in database. For activation of TagE route, the activation of TagE is most probable up-regulated the σ^F/σ^G in the forespore via RsbW/σ^B route (Figure 3.5A). Alternately, it will activate the PAS-RsbP gene and this route is only activated when the bacterium is exposured to cold shock at 37°C or lower. It was apparent that 65°C, this route was in dormant as observed by no protein expression at this temperature. There has also been reported that glucosyltransferase, TagE is an induce-cold response enzyme that functions in transcription repressed by PhoP~P under phosphate starvation conditions whereas its stress regulon is under control of the alternative transcription factor σ^B (75-77). For activation of YbbB route, protein expressions were observed to increase when the bacteria have undergone shock from 65°C. This is consistent to interpret that the up-regulation YbbB was able to activate the FeuA-RsbW route (Figure 3.5B), finally, leading to the σ^B production, which will subsequently convert to σ^F or σ^G in the forespore. For activation of RsfA route, it described the direct activation of RsfA to σ^F/σ^G in the forespore (Figure 3.5C). This route was activated only when the

bacteria were experiencing cold shock at 37°C and 25°C. There has also been reported that the activation of σ^F in the forespore leads to transcription of SpoIIR and SpoIIQ immediately after asymmetric division, and of several genes that can be disrupted without preventing formation of stress resistant spores and σ^G encoded SpoIIIG activates transcription in engulfed forespore of a large set of genes. (74,78) For activation of RsbT route, the RsbT route was only activated when the bacteria was experiencing shock at temperature lower than 37°C while the activation of this gene at 25°C is of unknown function (Figure 3.5D).

No direct route was established that this gene could involve in the production of σ^F/σ^G in the forespore and the additional proteins which were involved in the down stream of this route. However, there was report suggesting that RsbT also plays an important role for the coordinated expression of the σ^B factor that controls the general stress response in the vegetative cell cycle early sporulation of *Bacillus* sp. (79-83). RsbT is also a protein recognized as the upstream half of an operon of σ^B and it is responsible to be a regulator of σ^B activity, and the co-regulation of RsbS-RsbT pairs and RsbV-rsbW act hierarchically by a common mechanism in which key protein-protein interactions are controlled by phosphorylation events (82-86). Disruption of RsbU, or a deletion that removes RsbR, RsbS and RsbT, renders σ^B activity uninducible by environmental stress but still activatable by a drop in intracellular ATP (84, 87). In addition, σ^B activity in several RsbX strains with suppressor mutations in RsbT or –U was high during growth and underwent a continued, rather than a transient, increase following stress. Thus, RsbX is likely responsible for maintaining

low σ^B activity during balanced growth and for reestablishing σ^B activity at pre-stress levels following induction (87-88).

For deactivation of MrpA and PyrC routes, both proteins encoded genes MrpA and PyrC were down-regulated when the bacteria were experiencing shock at 37°C or lower. Neither MrpA nor PyrC was observed at 65°C, referring to the possibility that both genes were in the dormant mode in this temperature (Figure 3.5E). MRP protein homolog, MrpA, functions multi-resistance and pH homeostasis as Na^+/H^+ antiporter that affect post-translational regulational control of σ^H in the early sporulation of cell cycle (89, 90). Finally, the activation and deactivation of cold shock-induced proteins correlating to the σ^F/σ^G production in the forespore are summarized in Figure 3.6. Forespore is considered a proceeding event of sporulation of the bacteria when it undergoes cold stress. In this report, the protein expressions in the TagE, YbbB, RsfA and RsbT routes were activated when the bacterium temperature was dropped below the optimum at 65°C.

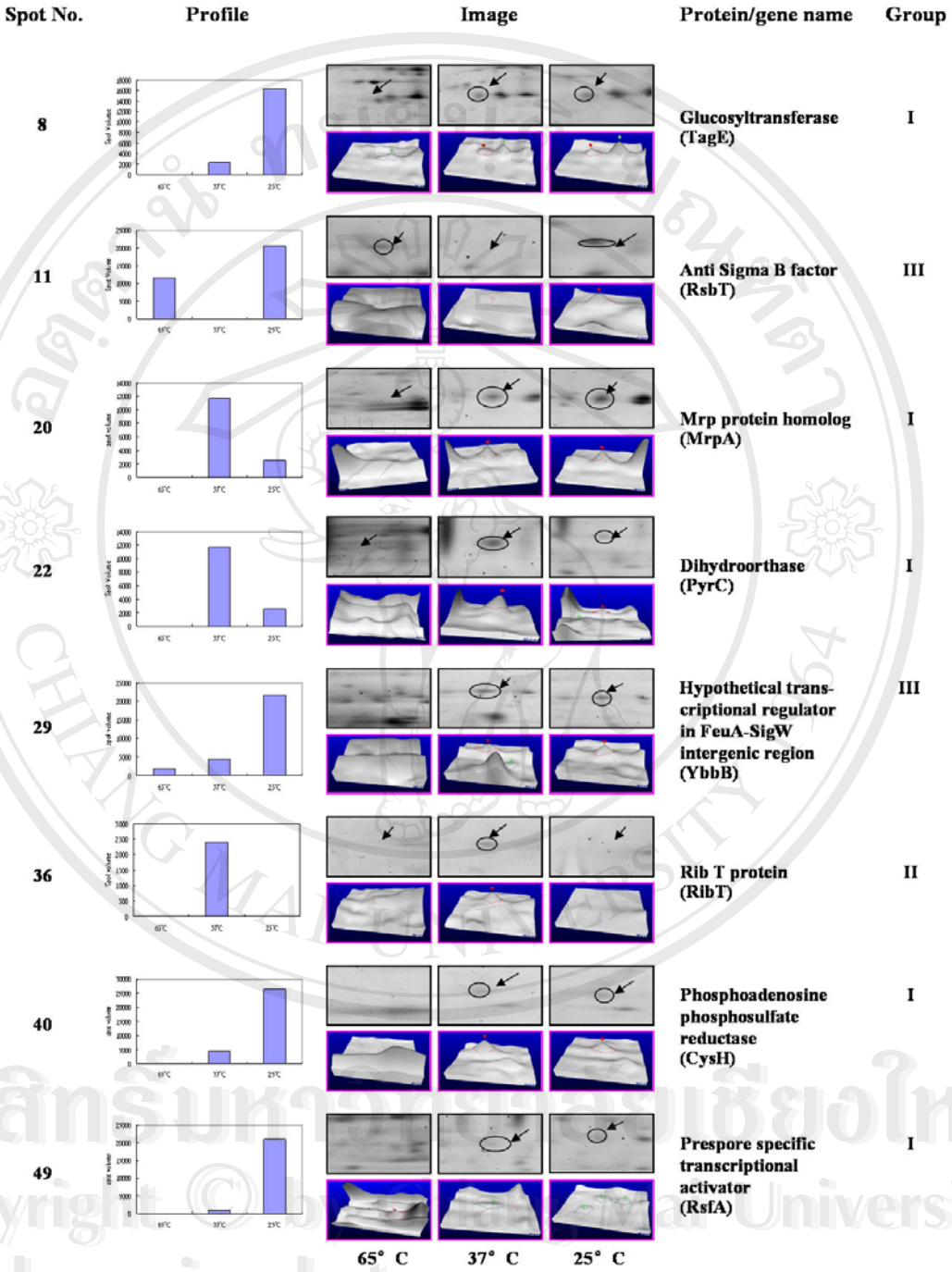

Figure 3.4 The 2-D and 3-D viewings of 8 major different proteins under cold shock stress analyzed by ImageMaster 2D.

Table 3.1 Protein identification of cytosolic proteins in *B. stearothermophilus* TLS33 after downshift temperatures to 37°C and 25°C The information of protein and gene names, description and functional category was searched by SubtiList database supplemented with EMBL/GenBank/DDBJ databanks and COG database.

Spot no.	Protein name (ID) / Accession no.	Gene name/ Accession no.	MW (Da) / pI	Description	Functional category
1	Pts system, fructose-specific IIB component (EIIB-FRU) (Fructose-permease IIB component) (Phosphotransferase enzyme II, B component) (P18) (PTFB) / P26380	*lev*E / X56098	35051 / 4.37	PTS fructose-specific enzyme IIB component	Transport/binding proteins and lipoproteins
2	Stage III sporulation protein AE (S3AE) / P49782	*spo*IIIAE / U35252	39191 / 4.55	Mutants block sporulation after engulfment	Sporulation
3	Inosine-5'-monophosphate dehydrogenase (IMP dehydrogenase) (IMPDH) (IMPD) (Superoxide-inducible protein 12, SOI12) (IMDH) / P21879	*gua*B / X55669	39191 / 4.62	Inosine-monophosphate dehydrogenase	Metabolism and transport of nucleotides and nucleic acids (purine biosynthesis)
4	COMF operon protein 3 (CMF2) / P39147	*com*FC / Z18629	29901 / 4.76	Late competence gene	Transformation/competence
5	Unknown	-	28100 / 4.64	-	-
6	Flagellar protein (FLIT) / P39740	*fli*T / Z31376	58100 / 4.64	Flagellar protein	Mobility and chemotaxis
7	DNA topoisomerase I (Omega-protein) (Relaxing enzyme) (Untwisting enzyme, Swivelase) (TOP1) / P39814	*top*A / L27797	58250 / 4.55	DNA topoisomerase I	DNA packing and segregation / DNA replication, recombination

Table 3.1 (continued)

Spot no.	Protein name (ID) / Accession no.	Gene name/ Accession no.	MW (Da) / pI	Description	Functional category
8	Probable poly (glycerol-phosphate) alpha-glucosyltransferase (Teichoic acid biosynthesis protein) (TAGE) / P13484	*tag*E / X15200	48700 / 4.44	UDP-glucose: polyglycerol phosphate glucosyltransferase	Cell wall
9	Translation initiation factor (IF-2) / P17889	*inf*B / M34836	48100 / 4.64	Initiation factor IF-2 (GTPase)	Initiation, Translation factors and enzymes involved in translation
10	Putative peptidase in gcvT-spoIIIAA intergenic region (YQHT) / P54518	*yqh*T / D84432	36067 / 5.10	Unknown; similar to Xaa-Pro dipeptidase	Protein modification
11	Anti-sigma B factor (RSBT) / P42411	*rsb*T / L35574	34803 / 5.14	Positive regulator of sigma-B activity (switch protein/serine-threonine kinase)	Adaptation to atypical conditions
12	Extragenic suppressor protein suhB homolog (SUHB) / Q45499	*suh*B / AF012285	31533 / 5.20	Archaeal fructose-1,6-biphosphate and related enzyme of inositol monophosphatase family	Carbohydrate transport and metabolism
13	Unknown	-	33103 / 5.30	-	-
14	Hypothetical 28.6 kDa protein in recQ-cmk intergenic region precursor (YPBG) / P50733	*ypb*G / L47648	34187 / 5.53	Unknown; similar to unknown proteins	From other organisms
15	Unknown	-	24187 / 5.53	-	-

Table 3.1 (continued)

Spot no.	Protein name (ID) / Accession no.	Gene name/ Accession no.	MW (Da) / pI	Description	Functional category
16	GTP-binding protein (LEPA) / P37949	*lep*A / X91655	69284 / 5.49	GTP-binding protein	Elongation
17	2,3-Bisphosphoglycerate-independent phosphoglycerate mutase (Phosphoglyceromutase) (BPG-independent pgaM) (Vegetative protein 107, VEG107) (LEPA) / P39773	*pgm* / L29475	69284 / 5.61	Phosphoglycerate mutase	Carohydrate transport and metabolism (gluconeogenesis)
18	Unknown	-	69486 / 5.72	-	-
17	2,3-Bisphosphoglycerate-independent phosphoglycerate mutase (Phosphoglyceromutase) (BPG-independent pgaM) (Vegetative protein 107, VEG107) (LEPA) / P39773	*pgm* / L29475	69284 / 5.61	Phosphoglycerate mutase	Carohydrate transport and metabolism (gluconeogenesis)
18	Unknown	-	69486 / 5.72	-	-
19	Peptide methionine sulfoxide reductase (Protein-methionine-s--oxide reductase) (Peptide met (O) reductase) (MSRA) / P54154	*msr*A / L77246	69284 / 5.81	Peptidyl methione sulfoxide reductase	Detoxification, Posttranslational modification, protein turnover, chaperone
20	MRP protein homolog (MRP) / P50863	*mrp* / X74737	28628 / 5.55	Multiple resistance and pH hemostasis	Transport/binding proteins

Table 3.1 (continued)

Spot no.	Protein name (ID) / Accession no.	Gene name/ Accession no.	MW (Da) / pI	Description	Functional category
21	Hypothetical 58.2 kDa protein in kdgT-xpt intergenic region (YPWA) / P50848	*ypw*A / L47838	38614 / 5.59	Unknown; similar to carboxypeptidase	Metabolism of amino acids and related molecule
22	Dihydroorotase (Dhoase) (PYRC) / P25995	*pyr*C / BG10714	39144 / 5.66	Dihydroorthase (Pyrimidine biosynthesis)	Metabolism of nucleotides and nucleic acids
23	Transcription antitermination protein nusG (NUSG) / Q06795	*nus*G / D13303	31924 / 5.63	Transcription antitermination factor	Termination
24	Ferrichrome transport ATP-binding protein (FHUC) / P49938	*fhu*C / X93092	33229 / 5.67	Ferrichrome ABC transporter (ATP-binding protein)	Transport/binding proteins and lipoproteins
25	Protein export protein prsA precursor (PRSA) / P24327	*prs*A / X57271	30331 / 5.85	Protein secretion (post-translocation molecular chaperone), phosphoribosylpyrophosphate synthetase	Protein secretion, nucleotide and amino acid transport and metabolism
26	Unknown	-	32802 / 6.16	-	-
27	Amidotransferase hisH (HIS5) / O34565	*his*H / AF017113	35465 / 5.84	Amidotransferase	Amino acid transport and metabolism (histidine biosynthesis)

Table 3.1 (continued)

Spot no.	Protein name (ID) / Accession no.	Gene name/ Accession no.	MW (Da) / pI	Description	Functional category
28	Hypothetical 35.0 kDa protein in rapJ-opuAA intergenic region (YCEB) / O34504	*yce*B / AB00617	43485 / 5.75	Unknown; similar to unknown proteins	From other organisms
29	Hypothetical transcriptional regulator ybbB in feuA-sigW intergenic region (ORF3) (YBBB) / P40408	*ybb*B / L19954	57121 / 4.55	Unknown; similar to transcriptional regulator (AraC/XylS family)	Regulation
30	Unknown	-	58250 / 6.07	-	-
31	Glycine betaine/carnitine/choline transport ATP-binding protein opuCA (OPCA) / O34992	*opu*CA / AF009352	54178 / 5.85	Glycine betaine/carnitine/choline ABC transporter (ATP-binding protein)	Transport/binding proteins and lipoproteins
32	Penicillin-binding protein 1A/1B (PBP1) [Includes: penicillin-insensitive transglycosylase (Peptidoglycan Tgase); Penicillin-sensitive transpeptidase (DDtranspeptidase) (PBPA) / P39793	*pon*A / U11883	49081 / 6.01	Penicillin-binding proteins 1A/1B	Cell wall
33	PBSX phage terminase small subunit (XTMA) / P39793	*xtm*A / Z70177	43484 / 6.14	Phage PBSX terminase (small subunit)	Phage-related functions, DNA replication, recombination and repair
34	Probable amino-acid ABC transporter ATP-binding protein in bmrU-ansR intergenic region (YQIZ) / P54537	*yqi*Z / D84432	29604 / 6.05	Unknown; similar to amino acid ABC transporter (ATP-binding protein)	Transport/binding proteins and lipoproteins

Table 3.1 (continued)

Spot no.	Protein name (ID) / Accession no.	Gene name/ Accession no.	MW (Da) / pI	Description	Functional category
35	Hypothetical 19.1 kDa protein in sigD-rpsB intergenic region precursor (ORFC) (YLXL)	ylxL / Z99112	32236 / 6.30	Unknown; similar to unknown proteins	From *B. subtilis*
37	PAL-related lipoprotein precursor (SLP) / P39910	*slp* / M57435	18200 / 4.77	Small peptidoglycan-associated lipoprotein, starvation-inducible outer membrane lipoprotein	Transport/binding proteins and lipoproteins, cell envelope biogenesis, outer membrane
38	Hypothetical protein YVYF (YVYF) / P39807	*yvy*F / Z99122	17648 / 5.15	Unknown; similar to unknown proteins	From *B. subtilis*
39	Unknown	-	12806 / 5.44	-	-
40	Phosphoadenosine phosphosulfate reductase (PAPS reductase, Thioredoxin dependent) (PADOPS reductase) (3'-Phosphoadenylsulfate reductase) (PAPS sulfotransferase) (CYH1) / P94498	*cys*H / U76751	22031 / 5.95	Phosphoadenosine phosphosulfate	Amino acid transport and metabolism, coenzyme metabolism (FAD biosynthesis)
41	Unknown	-	20546 / 6.05	-	-
42	Hypothetical 73.2 kDa protein in sodA-comGA intergenic region (YQGS) / P54496	*yqg*S / D84432	38549 / 6.14	Unknown; similar to putative molybdate binding protein	From other organisms

Table 3.1 (continued)

Spot no.	Protein name (ID) / Accession no.	Gene name/ Accession no.	MW (Da) / pI	Description	Functional category
42	Hypothetical 73.2 kDa protein in sodA-comGA intergenic region (YQGS) / P54496	*yqg*S / D84432	38549 / 6.14	Unknown; similar to putative molybdate binding protein	From other organisms
43	Aspartokinase 2 (Aspartokinase II) (Aspartate kinase 2) [contains: aspartokinase II alpha subunit; Aapartokinase II beta subunit] (AK2) / P08495	*lys*C / J03294	40764 / 6.32	Aspartokinase II (alpha and beta subunits)	Amino acid transport and metabolism (threonine and methionine biosynthesis)
44	Hypothetical 45.3 kDa protein in prkA-cspB intergenic region (ORF4) (YHBH)/ P45742	*yhb*H / Z99108	43986 / 5.25	Ribosome-associated protein Y (PSrp-1)	Translation, ribosomal structure and biogenesis
45	Unknown	-	56284 / 5.35	-	-
46	Hypothetical 17.9 kDa protein in nprE-pycA intergenic region (YLAL) / O07636	*yla*L / Z99111	18200 / 4.77	-	-
47	Stage III sporulation protein AH / P49785	*spo*IIIAH / Z99116	17587 / 5.64	-	-
48	(D49467) Unnamed protein product / BAA24873	-	56667 / 5.20	Unknown; similar to flagellar protein	Mobility and chemotaxis
49	Prespore specific transcriptional activator (RSFA) / P39650	*rsf*A / X73124	58758 / 5.34	Probable regulator of transcription of sigma-F-dependent genes, leucine zipper motif	Sporulation

Table 3.1 (continued)

Spot no.	Protein name (ID) / Accession no.	Gene name/ Accession no.	MW (Da) / pI	Description	Functional category
50	Glucose-6-phosphate isomerase (GPI) (Phosphoglucose isomerase) (PGI) (Phosphohexose isomerase) (PHI) (Vegetative protein 54) (VEG54) (G6PI) / P80860	*pgi* / Z93936	58515 / 5.52	Glucose-6-phosphate isomerase	Carbohydrate transport and metabolism (glycolysis, gluconeogenesis)
51	Unknown	-	20249 / 5.07	Unknown; similar to phage-related protein	Phage-related functions
52	Hypothetical 21.0 kDa protein in lysS-mecB intergenic region (YACH) / P37569	*yac*H / D26185	17461 / 5.70	Unknown	-
53	Molybdopterin-gianine dinucleotide biosynthesis protein B (O31704) / O31704	*mob*B / AF012285	18445 / 5.87	Molybdopterin-guanine dinucleotide biosynthesis	Metabolism of coenzymes and prosthetic groups

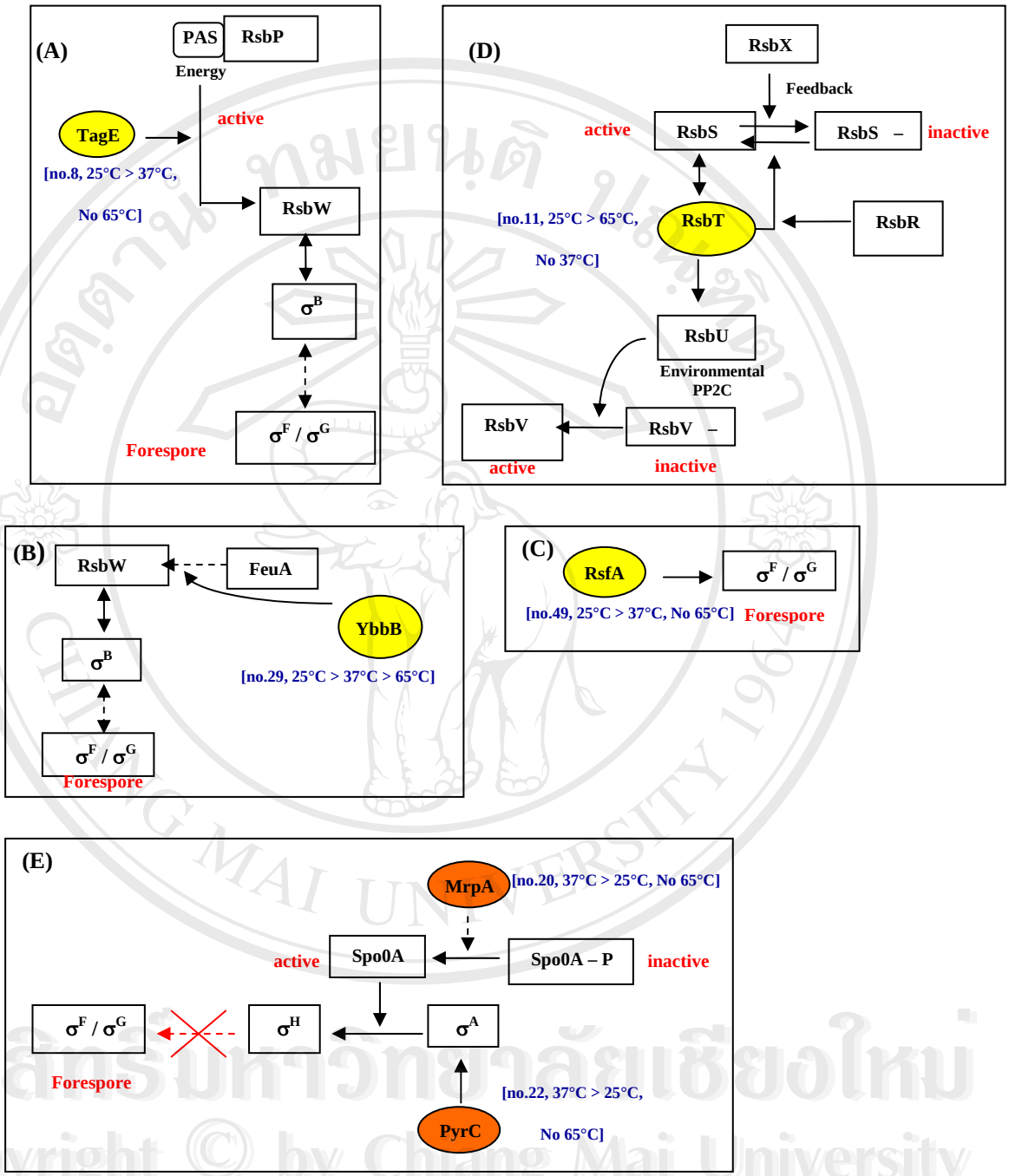

Figure 3.5. Activation and deactivation of signaling pathways to maintain the sporulation of *B. stearothermophilus* TLS33 under cold shock. (A) activation of TagE route (B) activation of YbbB route (C) activation of RsfA route (D) activation of RsbT route (E) deactivation of MrpA and PyrC routes.

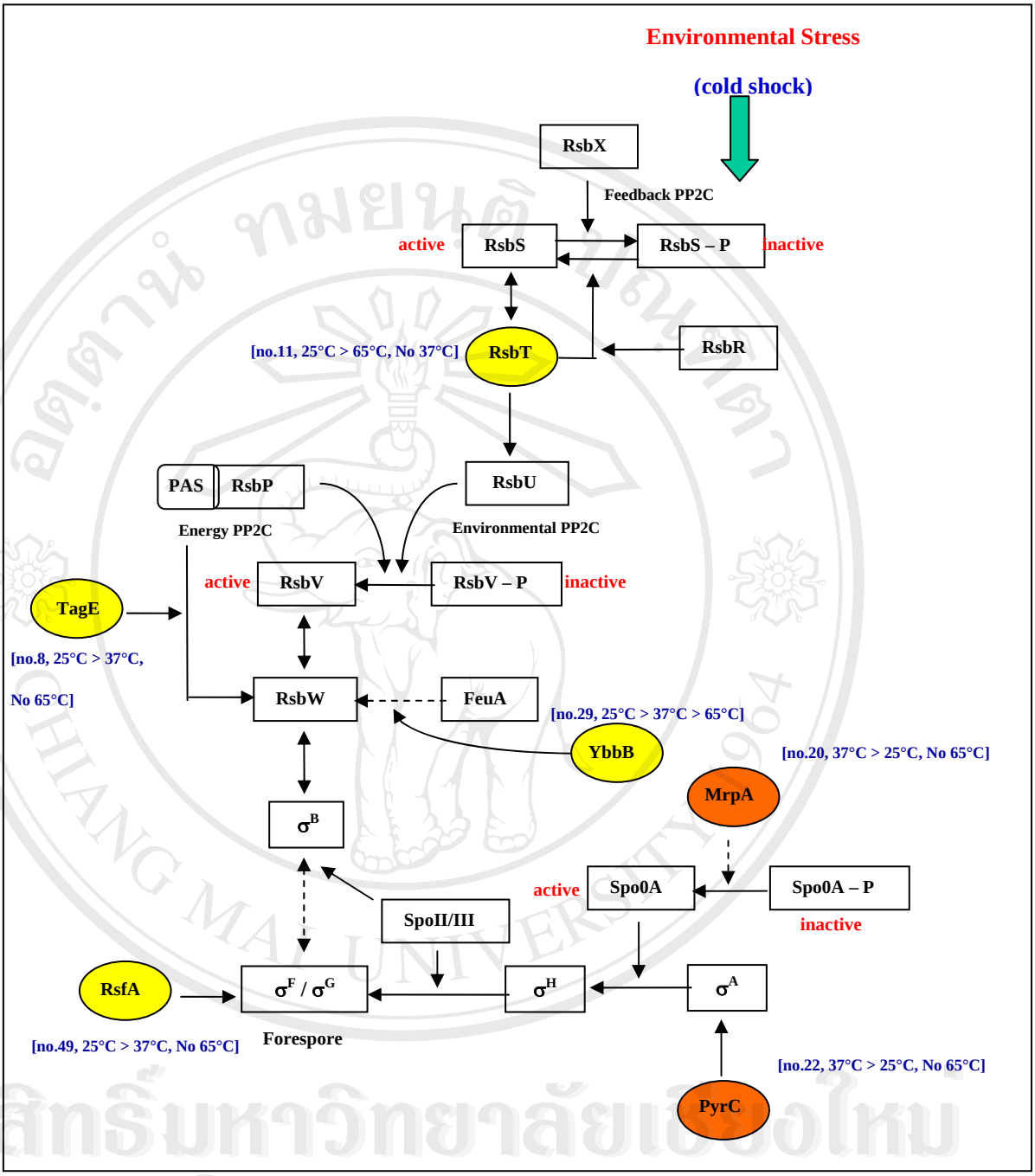

Figure 3.6 Summary of cold shock-induced proteins from *B. stearothermophilus* TLS33 correlated to the sporulation of signaling pathway under cold shock stress.

3.2 STRESS RESPONSES OF *BACILLUS STEAROTHERMOPHILUS* TLS33

3.2.1 Growth profiles in stress conditions

When challenged with the stress conditions during exponential growth, there was the assumption mentioned *B. stearthermophilus* TLS33 immediately stopped its growing (Figure 3.7, 3.8, 3.9). For 10% w/v salt stress, it was found that cell number of this bacterium was not increased. But in cold stress, the growth rate was slightly increased. In the case of 10% ethanol stress, the cell number was decreased in first two hours of the challenged stresses. However, the first two hours of individual stress conditions might result in changing in protein expression profiles. The studying on the protein expression profile in each stress conditions would be further investigated.

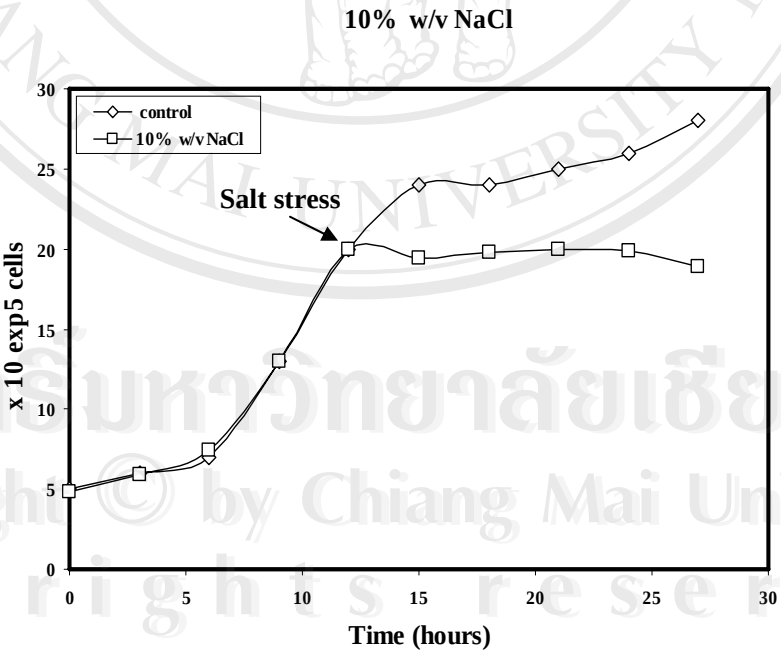

Figure 3.7 The growth profile of *B. stearothermophilus* TLS33 after salt stress

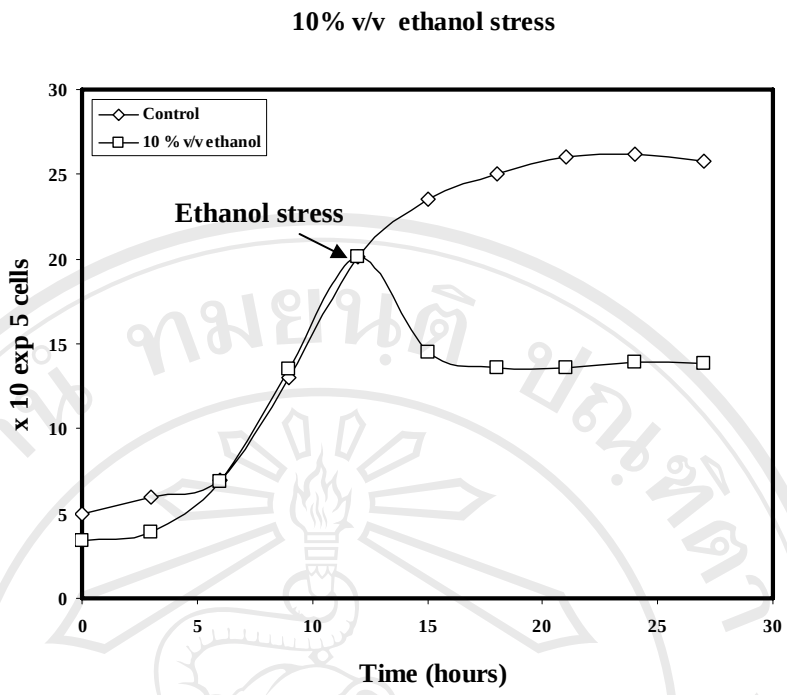

Figure 3.8 The growth profile of *B. stearothermophilus* TLS33 after ethanol stress

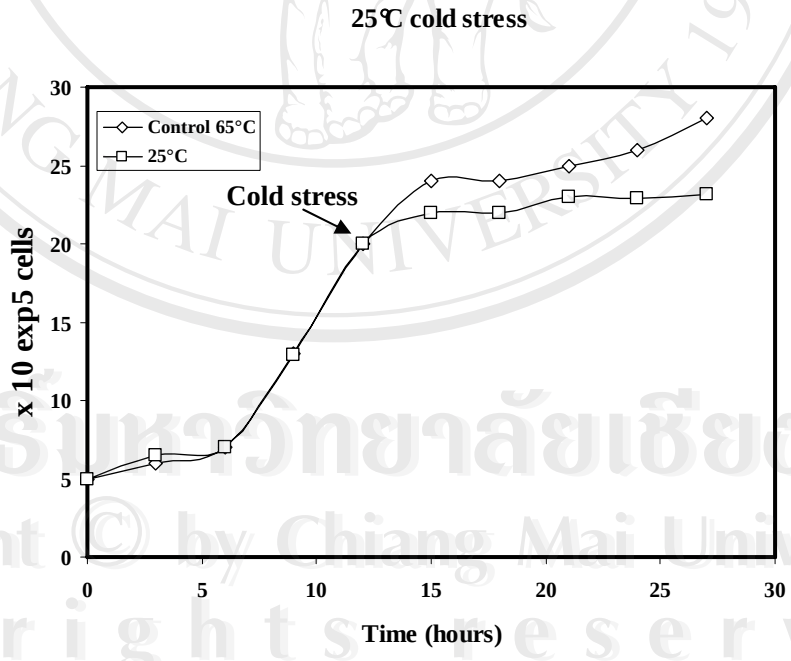

Figure 3.9 The growth profile of *B. stearothermophilus* TLS33 after cold stress

3.2.2 2DE, Image analysis and protein identification

From a physiological point of view, protein produced in response to stress is of crucial importance because stress is the rule and not the exception in natural ecosystems. The proteomes of non-growing cells are probably more heterogeneous than proteomes of growing cells. 2DE is a classical method for protein separation in proteomic field. Here, this method was applied for studying on stress responses of *B. stearothermophilus* TLS33. So far, PDQUEST 2 D analysis, Image analysis software, was used for analysis and generation of image and protein expression. After intracellular proteins were obtained from the stressed cell, they were separated with 2DE gels. The figure 3.10, 3.11 and 3.12 showed protein pattern in each stress condition and time point. Nevertheless, the proteins seem that they merely appeared on p*I* 4-7 region. So, IPG p*I* 4-7 stripes were applied in this study. Sypro Ruby stain provides the same sub-nanogram sensitivity as the best silver staining techniques and linear detection same as silver staining as well, after as little as 90 minutes of staining. No destaining is required to achieve high sensitivity and low background, and the gels can be left in the Sypro Ruby staining solution for indefinite periods without overstaining, vastly simplifying the simultaneous processing of multiple gels. Therefore, relatively good accuracy could be obtained from this stain. The 2DE images were acquired accurately from computerized imager of Typhoon scanner. This could indicate that they can analyze with image analysis software PDQUEST 2-D analysis. In this study, PDQUEST 2-D analysis is the software that was used for analysis of protein abundance. The intensity and size of the protein spots in the 2DE gel image indicated the up and down regulation of the protein spots. Whereby, this software normalized each gel to “housekeeping proteins”, filter out background noise,

and create virtual gels using Ideal Gaussian Representations of experimental gels. In addition, this software allowed statistical analysis of gels to determine which differences were significant and which were not. This thermophilic bacterium have been stressed with 25°C cold-stress, 10% w/v NaCl stress and 10% v/v ethanol stress. Subsequently, the intracellular proteins in each time course of each stress conditions were separated with 2DE gel for protein separation. After that, 2DE gels were stained with Sypro Ruby are able to provide the linear detection of proteins with good sensitivity as high as silver stain which provides the range in 4 ng to 8 ng of protein. Because of good linear detection of protein of Sypro Ruby, its application for protein staining so that it can provide reliability of investigation of differential protein expression in individual stress condition

The scatter plot graphs in figure 3.12, 3.14 and 3.15 demonstrated protein expressions in individual stress condition of this bacterium. These scatter plots were a tool for investigating differential protein expression. The three lines in graph represented level of changing protein abundant in 2DE gels. Normally, the software will set the X-axis to be reference gel and Y-axis to be slave gel or a gel which have to be compared with the reference gel. Thus, the above line indicates protein spots which are up-regulated up to 3 fold. On the other hand, below line also indicated protein spots which were down-regulated at least 3 fold. The middle line is regression line indicated the statistic of calculation from the software.

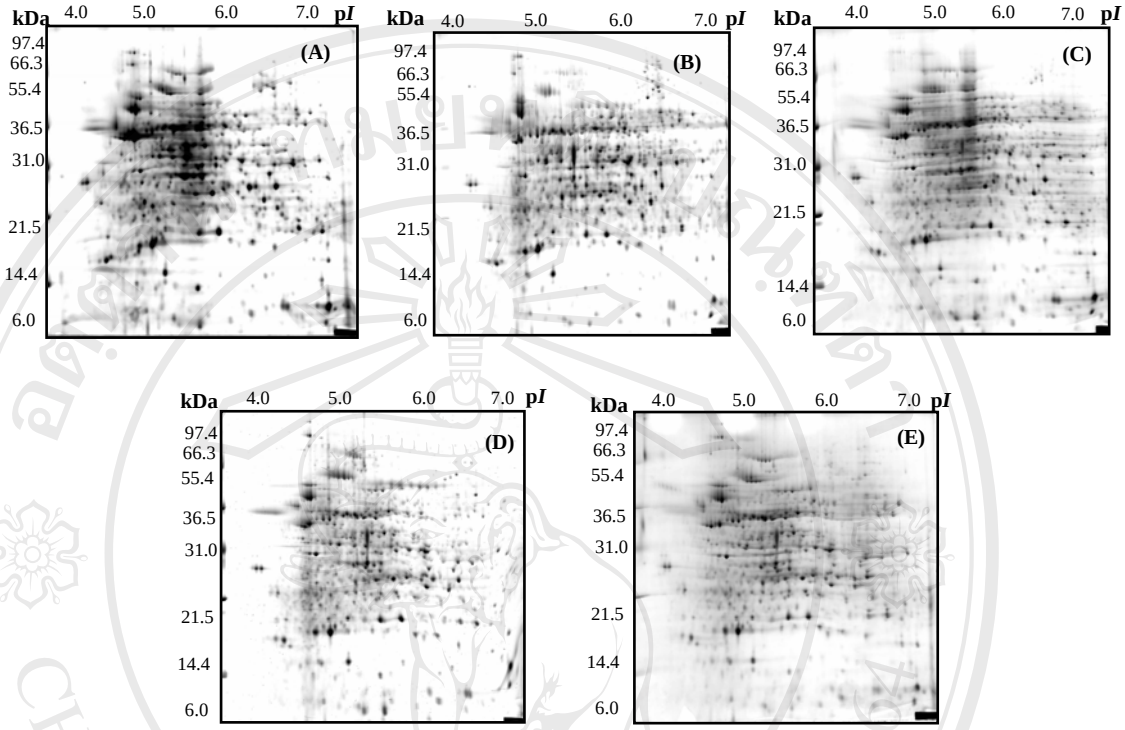

Figure 3.10 2DE gel image of *B. stearothermophilus* TLS33 proteins in salt stress (10% w/v NaCl). (A) , (B), (C), (D) and (E) are 2DE gel image of the intracellular proteins of the bacterium in 0, 30, 60, 90 and 120 minutes after it under 10% w/v NaCl salt stress conditions respectively.

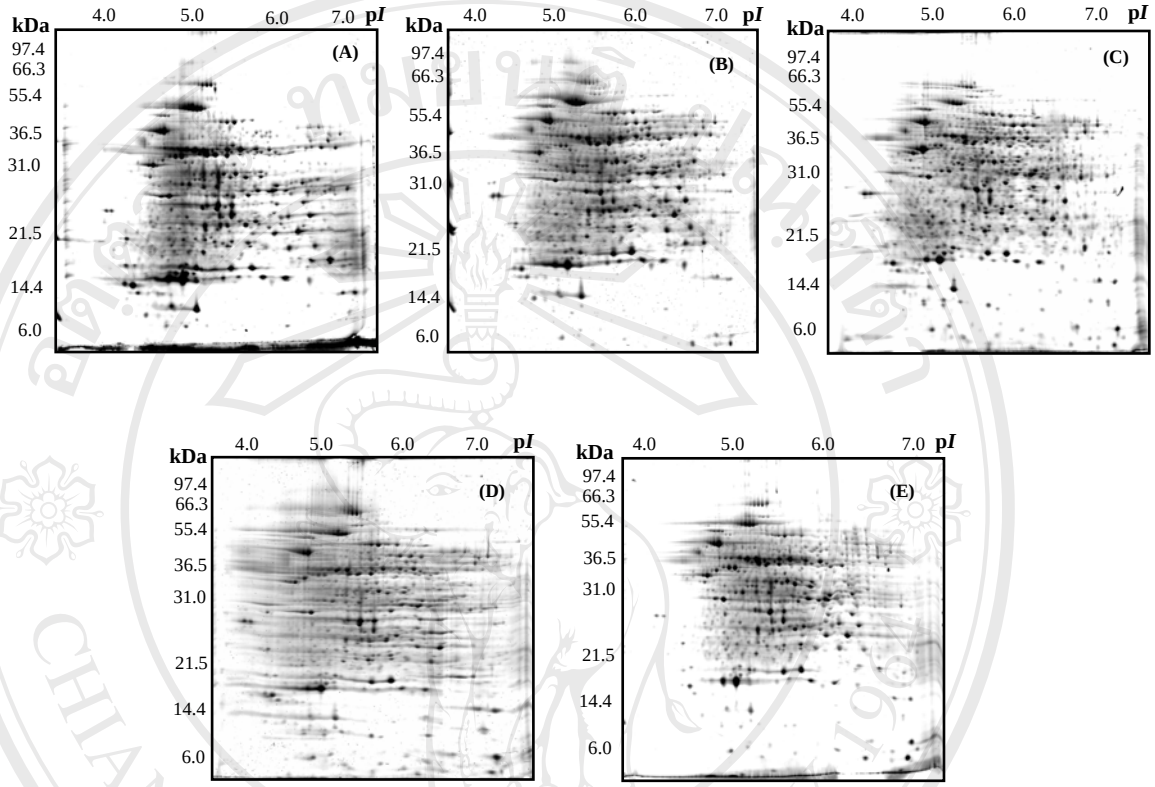

Figure 3.11 2DE gel image of *B. stearothermophilus* TLS33 proteins in 10% v/v ethanol. (A) , (B), (C), (D) and (E) are 2DE gel image of the intracellular proteins of the bacterium in 0, 30, 60, 90 and 120 minutes after it has been entered 10% ethanol stress conditions, respectively.

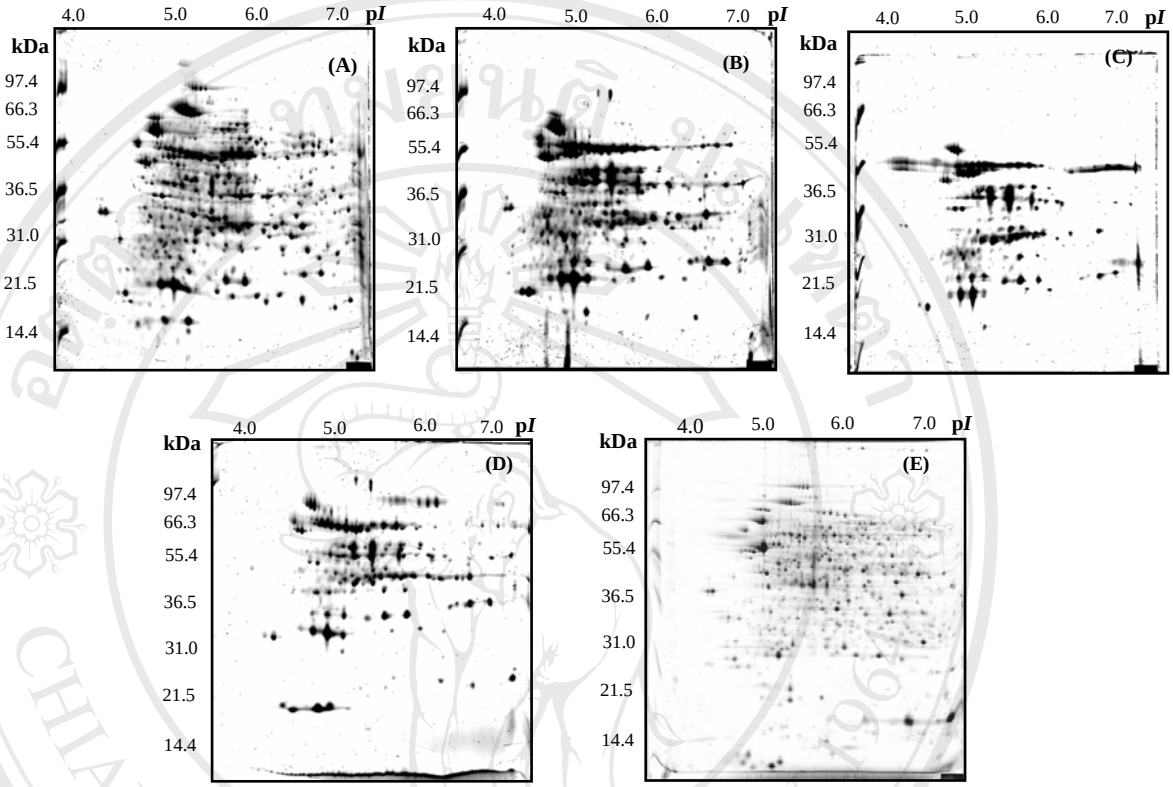

Figure 3.12 2DE gel image of *B. stearothermophilus* TLS33 proteins in 25°C cold stress (A) , (B), (C), (D) and (E) are 2DE gel image of the intracellular proteins of the bacterium in 0, 30, 60, 90 and 120 minutes after it has been entered 25°C cold stress conditions, respectively.

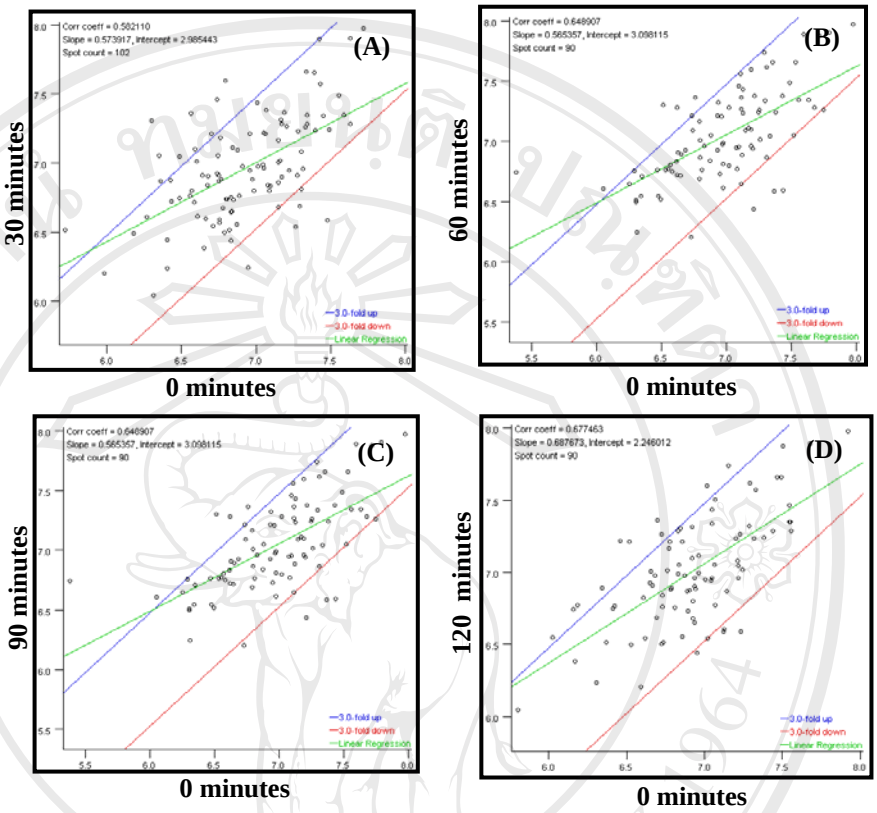

Figure 3.13 The scatter plot of 2DE-image analysis of salt stress of *B. stearothermophilus* TLS33. The image comparison was performed by each time points after stress was compared to 0 minutes after the bacterium has been stressed. (A), (B), (C) and (D) are the scatter plot of 30, 60, 90 and 120 minutes after stress compared to 0 minutes, respectively.

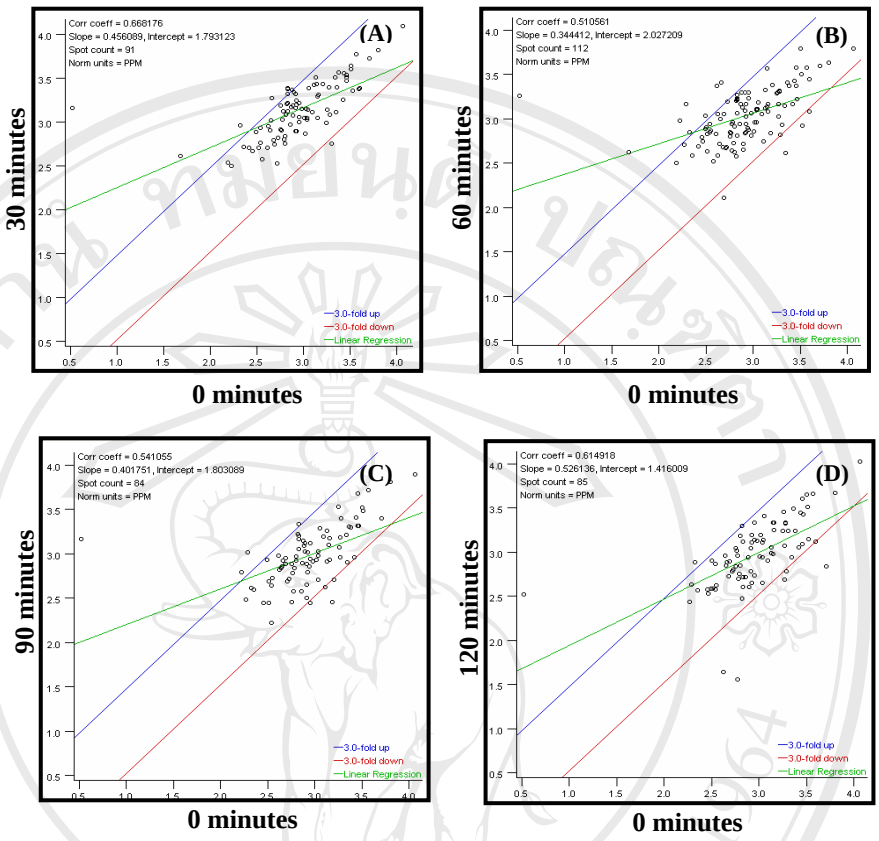

Figure 3.14 The Scatter plot of 2DE-image analysis of 10% ethanol stress of *B. stearothermophilus* TLS33. The image comparison was performed by each time points after stress was compared to 0 minutes after the bacterium has been stressed. (A), (B), (C) and (D) are the scatter plot of 30, 60, 90 and 120 minutes after stress compared to 0 minutes, respectively.

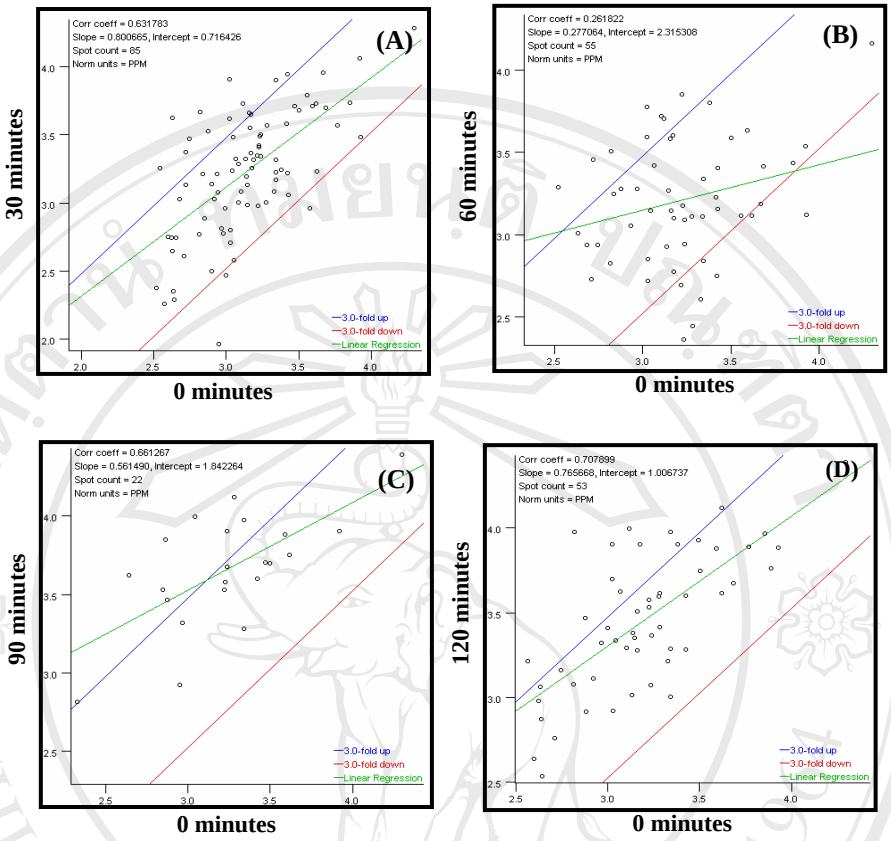

Figure 3.15 The Scatter plot of 2DE-image analysis of 25°C stress of *B. stearothermophilus* TLS33. The image comparison was performed by each time points after stress was compared to 0 minutes after the bacterium has been stressed. (A), (B), (C) and (D) are the scatter plot of 30, 60, 90 and 120 minutes after stress compared to 0 minutes, respectively.

3.2.3 Protein synthesis and protein level profiles in response in each stress condition.

After the 2DE gel image analysis, the interesting differential proteins were obtained. Subsequently, the differential proteins were characterized by using mass spectrometry. Thus far, MALDI-TOF MS is a method used for analyzing the molecular weight of tryptic digested peptide from individual differential protein spots. Nevertheless, resulting from limitation of 2DE and MALDI-TOF MS including post-translational modification of the proteins, a number of interesting protein spots could not be identified. However, there was an attempt to investigate changes of protein expression in each time course and subsequently identify them.

3.2.3.1 Protein level profiles in salt stress

The figure 3.16 has demonstrated the changing proteins in each stress condition at different times under salt stress. Among a number of changing proteins, GroEL has been found that it was changing during salt stress. GroEL is a chaperone protein which functions as protein folding and acts as proteolytic enzyme. Although it can be visualized in all stress conditions. For other proteins, it was further found that the proteins involved in detoxification or anti-oxidant proteins were also observed in salt stress such as Tpx, an enzyme postulated to be able to react with other detoxifying protein that would be oxidized with reactive oxygen species (ROS) in the cell (91). Mn-SOD or manganese-superoxide dismutase, a protein function as convert H_2O_2 to water, were observed that it has been down-regulated in this condition. In addition, Universal stress protein seems to be up-regulated after 30 minutes after it has been

encountered salt stress conditions. And then it was decreased with 120 minutes. For PyrB or aspartate carbamoyltransferase has been decreased after the bacterium encountered salt stress in every time course.

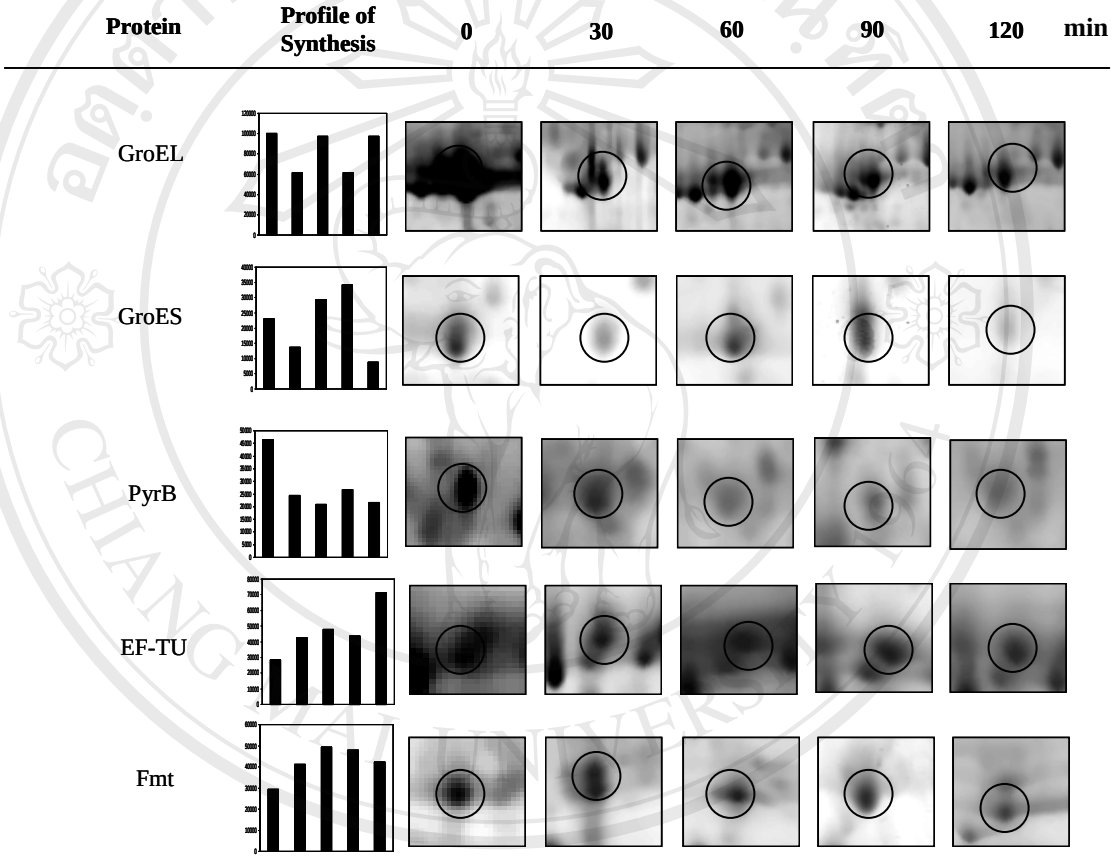

Figure 3.16 Synthesis and accumulation of some selected proteins in each different time of salt stress

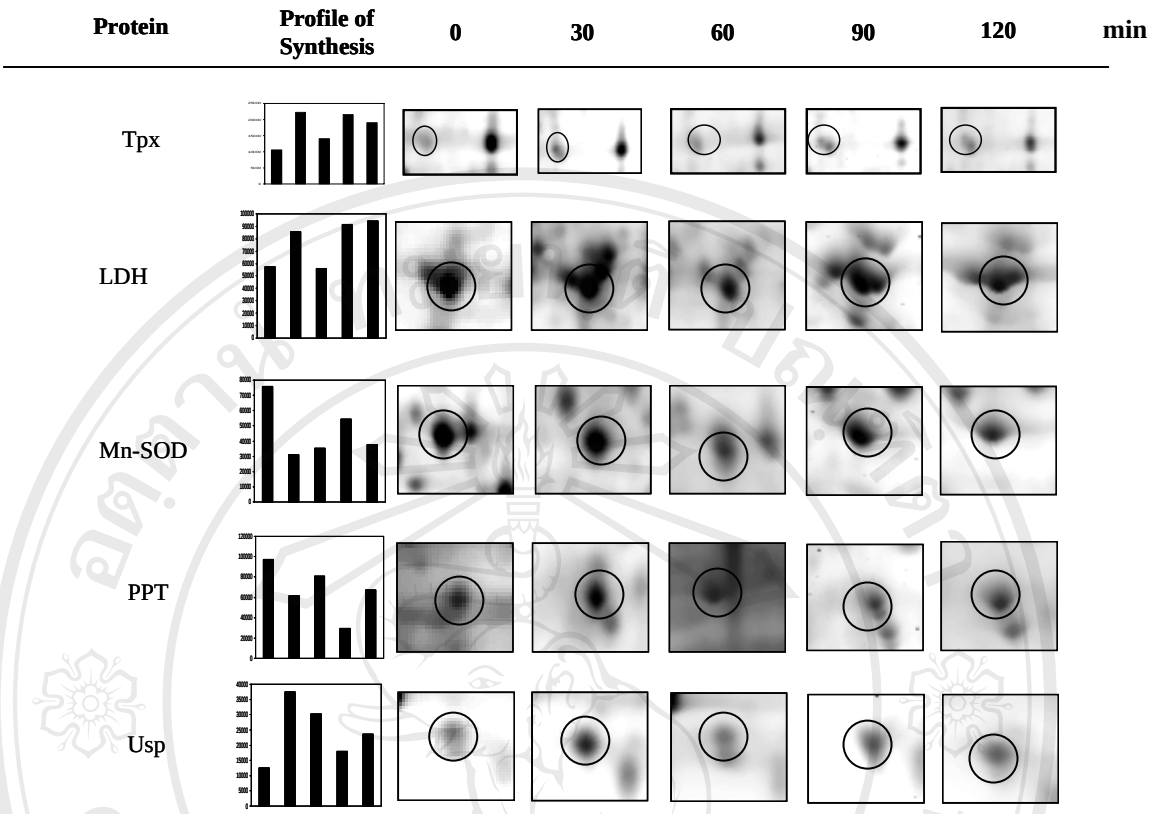

Figure 3.16(continued). Synthesis and accumulation of some selected proteins in each different time of salt stress

3.2.3.2 Protein level profiles in ethanol stress

When *B. stearothermophilus* TLS33 was has been encountered to 10% w/v ethanol stress, universal stress protein (Usp) has been also observed in this condition (Figure 3.17). This protein was expressed at every time points during this bacterium was under ethanol stress. Unlike, NADH dehydrogenase has been expressed after this thermophile encountered ethanol stress only 30 minutes. But, after that, this proteins

seemed to be decreased later. HrcA (transcription regulator of Heat Shock protein A) was strongly up-regulated within 60 minutes after ethanol stress. In general, HrcA functions as negatively regulate the transcription of heat shock genes which heat shock protein could be a stress protein in many organisms (92). Similar to salt stress, Tpx was up-regulated in ethanol stress as well. In this case, Tpx was decreased within 120 minutes after the bacterium was encountered ethanol stress. There were a number of studies reported that Tpx is a stress protein that when the bacterium was in unflavored conditions (93). Nevertheless, Tpx was also up-regulated in cold stress. For pyruvate dehydrogenase was increased until 90 minutes and was decreased within 120 minutes eventually. Many of reports have suggested that pyruvate dehydrogenase was used for NAD(P)H production which is a mechanism that can reduce ROS within the cell (94). Since ROS was believed that it can damage intracellular protein, membrane, lipid even nucleic acid such as DNA and RNA (95) Likewise, acetaldehyde dehydrogenase, ADH, is a protein in glycolytic pathway. It functions as changing acetaldehyde to ethanol. While this enzyme was working, consequently, its co-product also were produced in the meantime. This could suggested that the up-regulation of ADH aimed to produce NAD(P)H for useful reducing the ROS within the cell. ABC ATPase and Fmt or Met-tRNAi formyl transferase seemed to be up-regulated during the bacterium was under ethanol stress as well, but there was no the literatures could be supported this. Therefore, it is necessary to further investigate. However, 2DE might have limitations in protein complex. For example, very small protein or less than 5 kDa even very big protein could not be visualized. As well as the capacity of protein staining and detection were not able to be visualized low abundance protein. Including, extremely acid or basic proteins as well as hydrophobic

protein were hardly able to be separated by isoelectric focusing electrophoresis. This meant a number of proteins might be lost because of the limitation of the 2DE approach.

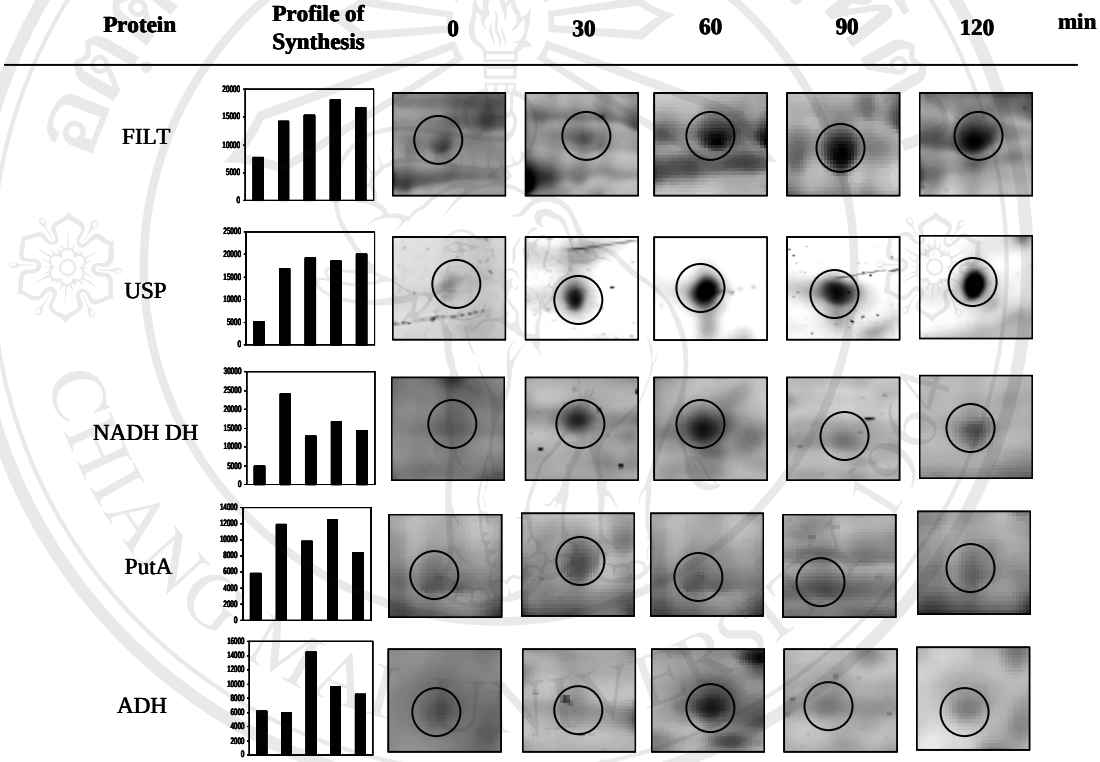

Figure 3.17 Synthesis and accumulation of some selected proteins in each different times of 10% v/v ethanol stress

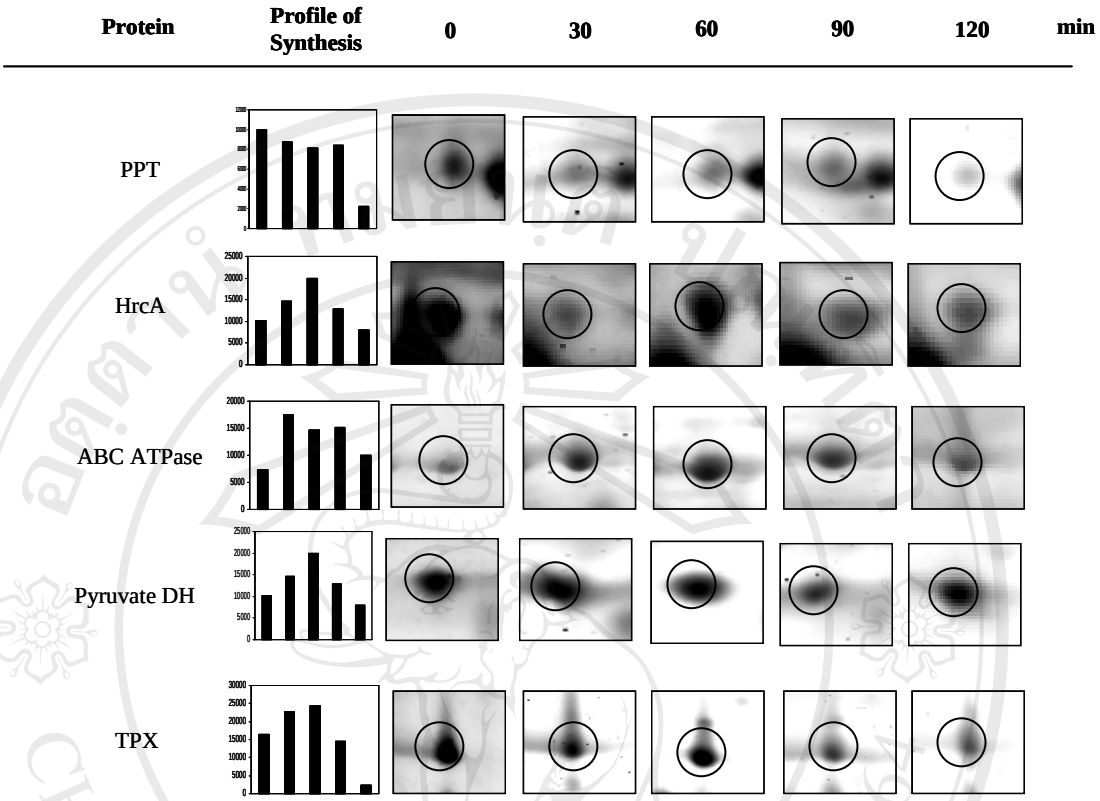

Figure 3.17 (continued) Synthesis and accumulation of some selected proteins in each different times of 10% v/v ethanol stress

3.2.3.3 Protein synthesis profiles in cold stress

In general, cold stress seemed to be a mild condition because it effected slightly on protein expression. However, CspB or cold shock protein B was strongly up-regulated when the bacterial culture was brought to lower temperature, 25°C. But the results showed that CspB was expressed in first 30 minutes after the bacterium

had been under 25°C. Whereas the previous report mentioned that this protein will be expressed at 4°C in *Bacillus subtilis* (96) (Figure 3.18).

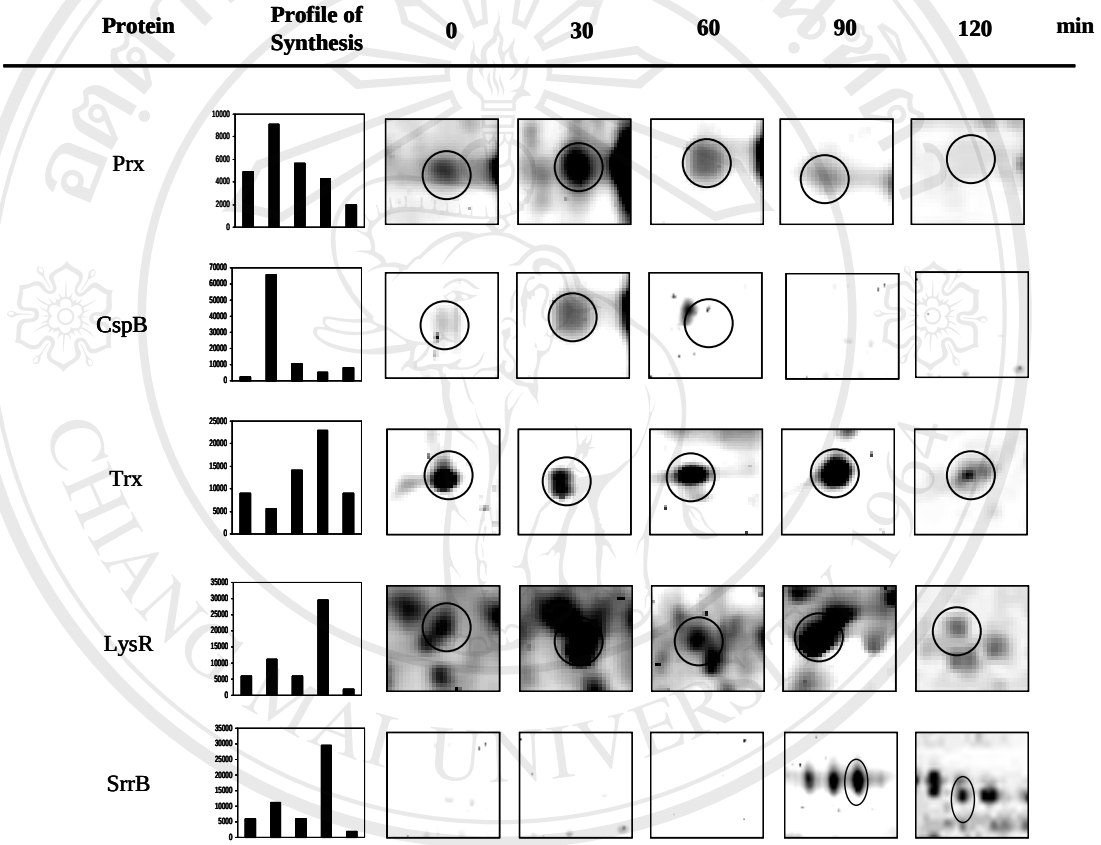

Figure 3.18 Synthesis and accumulation of some selected proteins in each different time of cold stress

Thus, this suggested that thermophiles also produce CspB likewise mesophiles but it might not produce this protein at very low temperature as the mesophiles. AhpC (alkyl hydrogen peroxidase) is a detoxifying protein which was up-regulated in first 30 minutes of cold stress and it was decreased after 90 minutes. The figure 3.18 has shown the changing in AhpC in acidic isoform. In addition, a number of reports mentioned that the shift of this protein to more acidic region in 2DE was resulted from it was modified in –SH in its cysteine residue and it subsequently was formed cysteic acid by ROS (61). Thioredoxin or TRX seemed as it was up-regulated after the bacterium was under cold stress until 90 minutes. TRX serves as detoxifying protein as well. This enzyme functions as oxidizing peroxiredoxin or AhpC which also has been observed in this stress. In addition, it has been decreased with 120 minutes. These findings could suggest that they functioned in different time course, although they work together (97). Both of LysR (transcription regulator LysR family) and SrrB (Sensor histidine kinase) were strongly induced by low temperature. It was observed that it most strongly induced within 90 minutes after it exposure to low temperature condition. LysR is a protein which serves as transcriptional regulator. While SrrB is protein, which involved in signal transduction pathway, acts as a sensor protein kinase. Overall, in each stress could induce protein in different pathway. However, as it has mentioned above, there were a number which could not be visualized by 2DE technique. Nevertheless the major up-regulated proteins were involved in oxidative stress. For example, Tpx and AhpC, they actually are the detoxifying proteins which have mentioned above. Thus, the proteomic analysis of this thermophile under oxidative stress was further analysis.

3.3) THE STUDYING ON POST-TRANSLATIONAL MODIFICATION OF AHPC OR PEROXIREDOXIN (PRX)

3.3.1 Bacterial survival of *B. stearothermophilus* TLS33 under oxidative stress

The survival of thermophile *B. stearothermophilus* TLS33 after treatment with different concentrations of H_2O_2 is shown in Fig. 3.19. In general, hydrogen peroxide produced the reactive oxygen species (ROS) which are generated aerobically by auto-oxidation of electron transport chain components and, when present in excess, can damage various components of living cells (98-99). Thus, the percentage of bacterial survival decreased from 100 to 85 %, approximately after addition of H_2O_2 from 50 to 500 μM, respectively. But at 10 μM of H_2O_2, it did not affected on the survival of this bacterium.

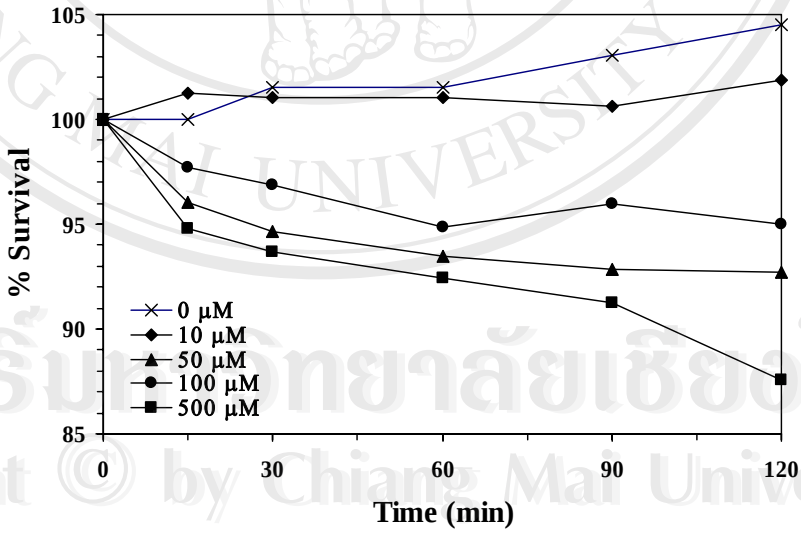

Figure 3.19. Survival percentage of *B. stearothermophilus* TLS33 after addition of different concentrations of H_2O_2 (10, 50, 100, 500 μM) along 120 minutes.

3.3.2 2-DE analysis of *Bacillus stearothermophilus* TLS33 cells and protein identification

Although the regulation in gene level of several bacteria under oxidative stress has been reported (66) the regulation in protein level including protein expression and post-translational modification are rarely studied in this bacterium. In order to more understand on the stress responses of *B. stearothermophilus* TLS33 under oxidative condition, the proteomic approach has been used for detection and identification of the proteins are differentially expressed against to oxidative stress within a short period time of 15 minutes. The 2-DE analysis of the intracellular proteins of *B. stearothermophilus* TLS33 demonstrated the protein patterns have been slightly altered (Figure 3.21). Interestingly, there were four isoform spots at the low molecular weight approximately 27 kDa were markedly changed corresponding to the concentration of H_2O_2. Consequently, the four spots were further analyzed by MALDI-TOF MS/MS and N-terminal sequence. It was found that these proteins were identified as peroxiredoxin (Prx). Due to it seemed to be changed corresponding to treated concentration of H_2O_2. Thus, they were denoted as Prx I, Prx II, Prx III and Prx IV from basic region to acidic region in 2DE, respectively. The probability-based scoring of the mass spectrums of peroxiredoxin isoforms derived from the calculation by Perkins *et al.* (100) informed the high scoring of mass database search which indicated that these four spots were peroxiredoxin reliably (Table 3.2). In addition, those isoforms Prx I, Prx II, Prx III and Prx IV appeared at the same molecular weight but different in p*I* with 5.0, 4.87, 4.81 and 4.79, respectively. It was suggested that a shift to a more acidic spot position may be caused by post-translational modification which might occur in response to oxidative stress when cysteine residues are oxidized

to sulfonic acid (101). Moreover, N-terminal sequence of these isoforms was determined in this study which is SLVGKKVQPFRAQAY.

In generally, peroxiredoxins are a ubiquitous family of antioxidant enzymes, which play an important role in many physiopathological processes, including adaptation to oxygen (102,103).

Table 3.2 Protein identification of four isoforms of Prx from *Bacillus stearothermophilus* TLS33.

Isoform	**MW (kDa)**	**p*I***	**Mowse Score**	**Peptide Matched No**	**Sequence Coverage (%)**	**Matching Sequence**
Prx I	27	5.00	347*	4	38	MFDVLDEEQGLAQR IEYVMIGDPSHQLSR AQAYHNGEFIEVTEQDFMGK GTFIIDPDGVIQAVEINADGIGR
Prx II	27	4.87	252*	4	27	
Prx III	27	4.81	80*	4	7	
Prx IV	27	4.78	131*	3	27	MFDVLDEEQGLAQR IEYVMIGDPSHQLSR GTFIIDPDGVIQAVEINADGIGR

*means the score indicate identity or extensive homology. (Protein scores are derived from MASCOT software.)

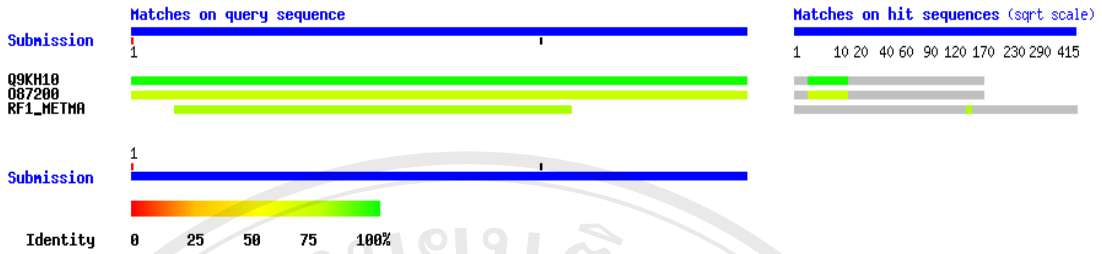

Figure 3.20 The identities of N-terminal sequence of Prx of *B. stearothermophilus* TLS33 against to other species by BLAST-P program.

Table 3.3 The identities of N-terminal sequence of Prx spots which was compared to other species by BLAST-P program.

Protein name	Species	N-terminal sequence	Identities
unknown	*Bacillus stearothermophilus* TLS33	SLVGKKVQPFRAQAY	100
Prx	*Thermus aquaticus*	SLVGKKVQPFRAQAY	100
AhpC	*Amphibacillus xylanus*	SLIGTEVQPFRAQAF	73

In the case of bacteria, the metabolic context of Prx and its physiological relevance have not yet been widely studied, especially the alteration of Prx isoform depending on the oxidative state. In our results, we are firstly found that thermophile *B. stearothermophilus* TLS33 produced the four Prx isoforms when encountered oxidative stress. In fact, Both of Prx I and II normally appeared in the cytosol of this bacterium. After addition of H_2O_2 and incubation for 15 min, Prx isoform were

shifted depending on the H_2O_2 concentration. This result was supported by the previous study which reported that the acidic form of peroxiredoxins was an oxidative modified form after organisms have encountered oxidative stress, whereas the basic form was the normal form of Prx (104). It was suggested that the reactive oxygen species (ROS) can oxidize the Prx and modify its –SH resulting in generation of four isoforms of Prx while the bacterium was under oxidative stress. Subsequently, Prx II, Prx III and Prx IV abundances were increased in the oxidative stress condition.

3.3.3 Acidic shift of peroxiredoxin isoform

Since peroxides are weak oxidizing agents, they can react with cysteinyl-thiols in proteins by formation of disulfide bonds or sulfonic acid derivatives (105). While cells are growing, significant amounts of O_2^- and H_2O_2 are generated by enzymatic misdirection of electrons to dioxygen. It is assumed that flavin-dependent transfer reactions of respiratory chain are primary responsible for generation of ROS. If the amount of ROS increases to toxic levels, cells encounter oxidative stress. In this study, we used H_2O_2 as an oxidative stressor to investigate the bacterial cells how they protected themselves from harmful conditions of oxidative stress. In order to conveniently visualization of the peroxiredoxin isoform appearance, 3-D viewings of peroxiredoxin area under different concentrations of H_2O_2 were generated by using ImageMaster™ 2D platinum software and used to examine alteration of peroxiredoxin (Fig. 3.22A). In addition, the volume of peak area in 3-D viewing of peroxiredoxin isoforms can be equivalent the protein intensity as shown in Fig. 3.22B. The image viewings showed Prx I normally located on basic region while Prx II, Prx III and Prx

IV located on acidic region. In the presence of different H_2O_2 concentrations, 2-D and 3-D viewings demonstrated the markedly difference in expression level of peroxiredoxin isoforms, which are dependent on the concentration of H_2O_2, especially at the high concentration of 500 μM. Interestingly, Prx III slightly appeared in the absence of H_2O_2 and in the low cysteines were oxidized and turned into cysteine sulfenic acid (105-107).

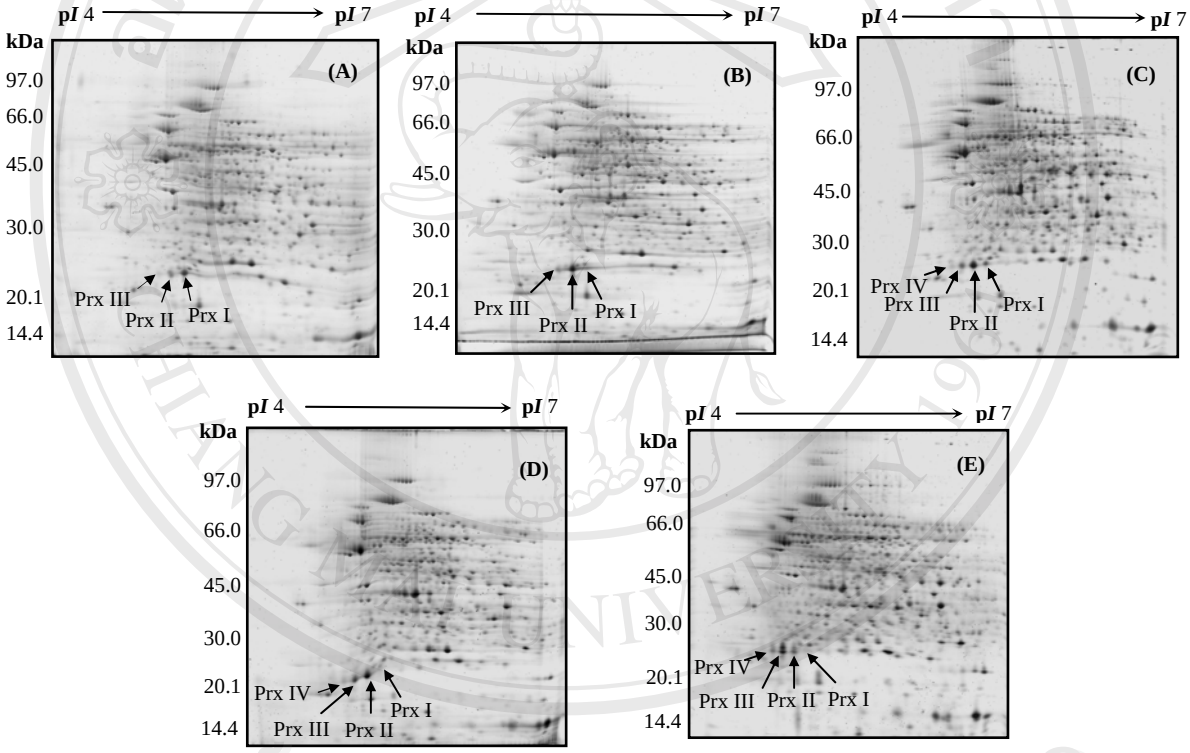

Figure 3.21 2-DE images of intracellular proteome of *B. stearothermophilus* TLS33 under oxidative stress. (A), (B), (C), (D) and (E) are the 2DE images of intracellular proteins after addition of 0 (Control), 10, 50, 100 and 500 μM of H_2O_2 for 15 min, respectively. The differentially expressed proteins under oxidative stress were analyzed by MALDI-TOF MS/MS. The different isoforms of peroxiredoxin are shown by the arrows.

(A)

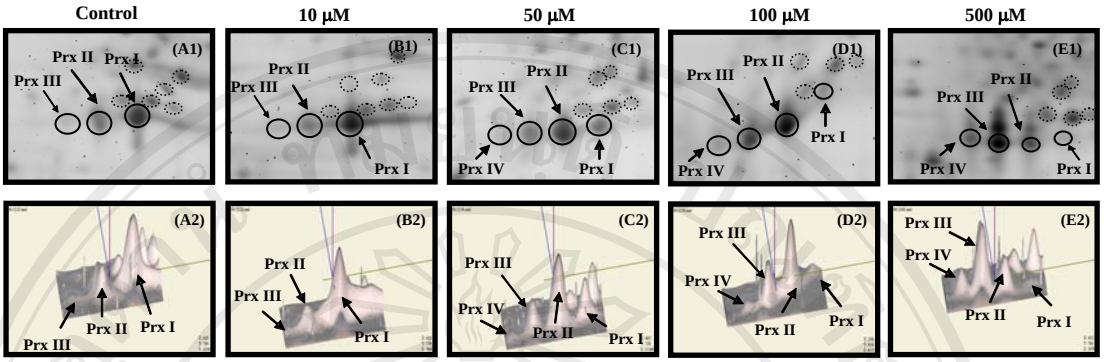

(B)

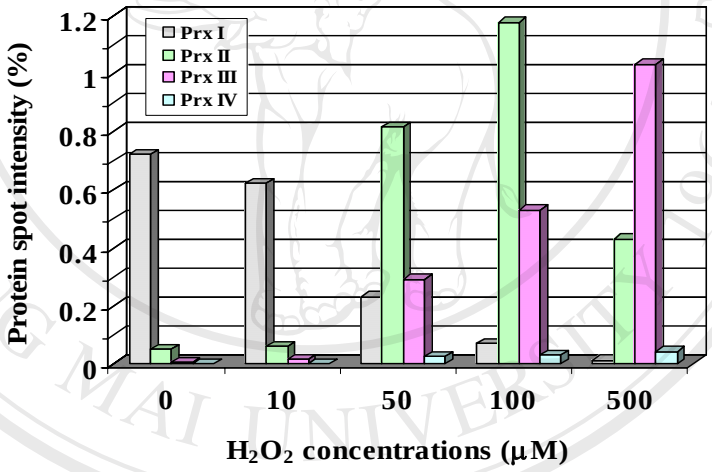

Figure 3.22 The peroxiredoxin (Prx) expression in *B. stearothermophilus* TLS33 under oxidative stress (A) 2-D and 3-D images covering the Prx isoforms region under individual concentration of H_2O_2 for 15 min. (A) , (B), (C), (D) and (E) are the Prx spots in 2DE gel and 3-D viewing of the individual sample was treated with 0, 10, 50, 100 and 500 μM of H_2O_2, respectively.

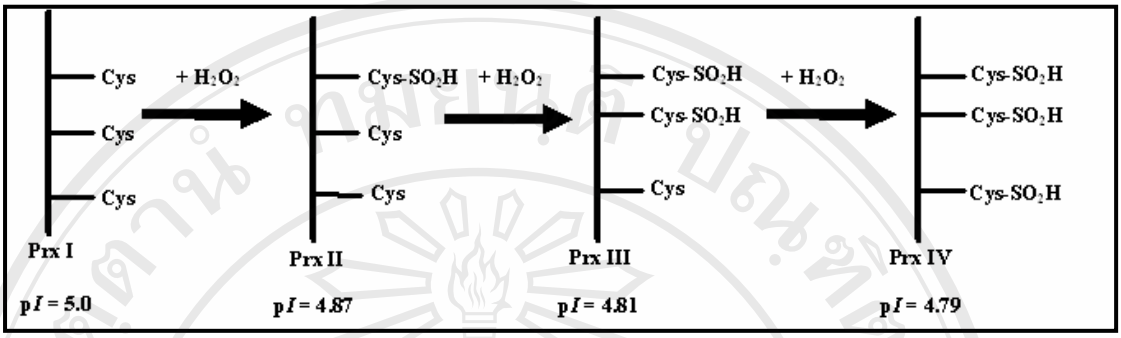

Figure 3.23 Hypothesis of *B. stearothermophilus* TLS33 Prx isoforms that are modified by H_2O_2. The modification of active site cysteines resulted in acidic shift of peroxiredoxin by forming the complex with sulfinic acid at active site residue.

Prx I was observed in the concentration of 10 μM H_2O_2 whereas Prx IV was no observed. The appearance of Prx III and Prx IV was occurred in the presence of 50 μM H_2O_2 condition and/or higher concentration of H_2O_2.

In the absence of H_2O_2, Prx I is the most abundant form. When the concentration of H_2O_2 was increased, it was found that the Prx I abundance was decreased whereas Prx II, Prx III and Prx IV abundances were subsequently increased (Fig. 3.22B). Thus, it was concluded that the Prx II, Prx III and Prx IV abundances were directly increased corresponding to the increase of concentration of H_2O_2.

3.3.4 Effect of stress time on modification of Prx isoforms under oxidative stress

According to the results of different concentration of H_2O_2, Prx II showed the most abundance at 100 μM of H_2O_2 and subsequently decreased at 500 μM of H_2O_2, while Prx III and Prx IV abundances were increased corresponding to the increase of H_2O_2 concentrations. At 120 minutes of stress period, Prx I abundance was decreased whereas Prx III abundance was increased. (Figure 3.24). Surprisingly, Prx IV eventually appeared in rather acidic region (p*I* 4.79) It was found that the oxidized forms of Prx were not reduced back to its original forms along 120 minutes. According to the previous reports, the oxidation of the active site cysteine to the sulfenic state has also been considered to be irreversible (96) Otherwise, the reversibility of Prx III to its original form (Prx I) is probably difficult because of the stability of sulfenic acid ($R\text{-}SO_2H$) which obtained from modification of cysteine residue, however, there was a study revealed that this protein could be reduced back by other enzyme (67). Nevertheless, it is necessary to further study that when H_2O_2 is absent in all surrounding conditions of bacterial cells, whether these proteins would be reduced and returned to its original form and there were any intracellular enzymes were able to reduce the oxidized Prx isoform. For this reason, the regulatory pathway of these proteins and other proteins under oxidative stress, which have the potential to be signaling proteins, is necessary to be further investigated. However, other thiol oxidized proteins will be investigated by using fluorescence dye, Cy3 Maleimide, labeling. This is the further study in this research.

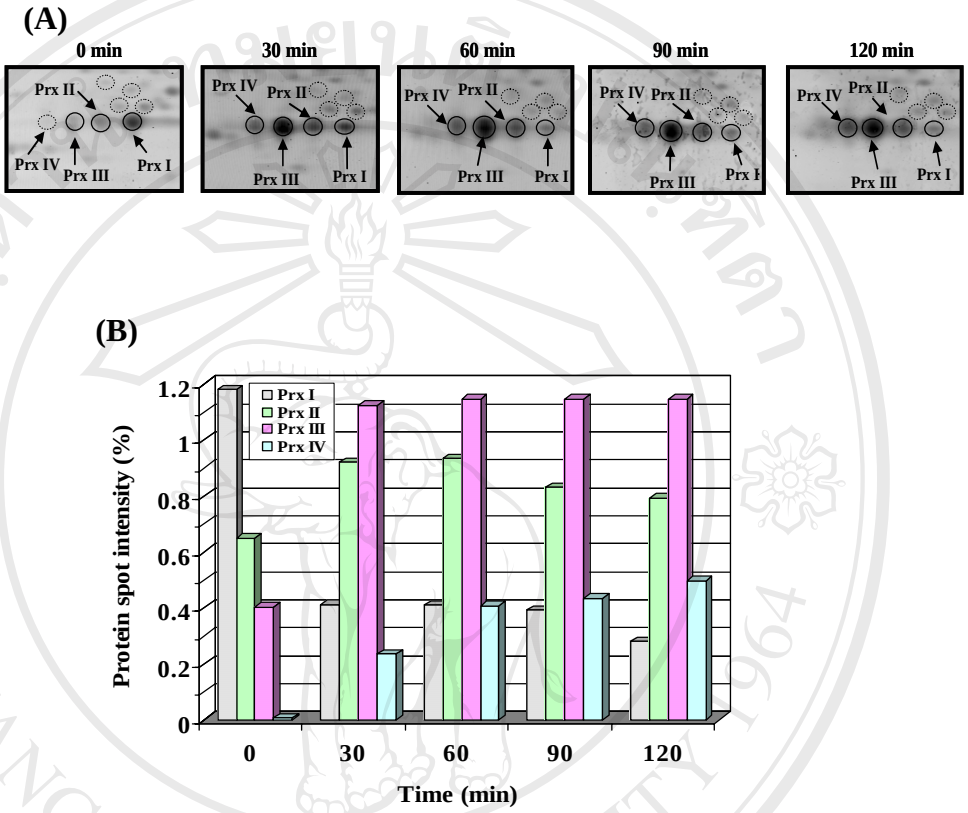

Figure 3.24 The Prx expression in *B. stearothermophilus* TLS33 under oxidative stress in different stressed times. (A) 2-DE images of peroxiredoxin isoforms in the presence of 500 μM H_2O_2 and different time points. (B) Percentage of protein spot intensity of Prx isoforms at different times after addition of 500 μM H_2O_2.

3.3.5 Post-translational modification by LC-MS/MS of Prx

To confirm the hypothesis, the Prx isoforms would be modified with ROS or H_2O_2 and formed sulfenic acid in cysteine residues (Cys-SO_2H). Subsequently, the original and more acidic spots were analyzed by LC-MS/MS. It was found 135 mass difference in the tryptic digested peptide 598 *m/z* from Prx II between ion b3 and b4. The 135 mass difference was derived from mass of O_2 (molecular mass 32) modified the Cysteine (molecular mass 103) (Figure 3.25). The H_2O_2 oxidized SH group of cysteine residue in Prx I and then it would shift to a more acidic region and formed Prx II. Furthermore, the mass different 135 were found in the tryptic digested peptide 598 *m/z* between ion b3 and b4 and 809 *m/z* peak between ion b6 and b7 from Prx III. Whereas it was found only in 598 *m/z* is present in Prx II. Thus, it has supported that –SH of Prx II was modified at another its active –SH (Figure 3.23) and resulted in forming Prx III because the 809 *m/z* peak was found mass difference whereas it could not be found in Prx II. For Prx IV, it could not be found the 135 unit mass difference

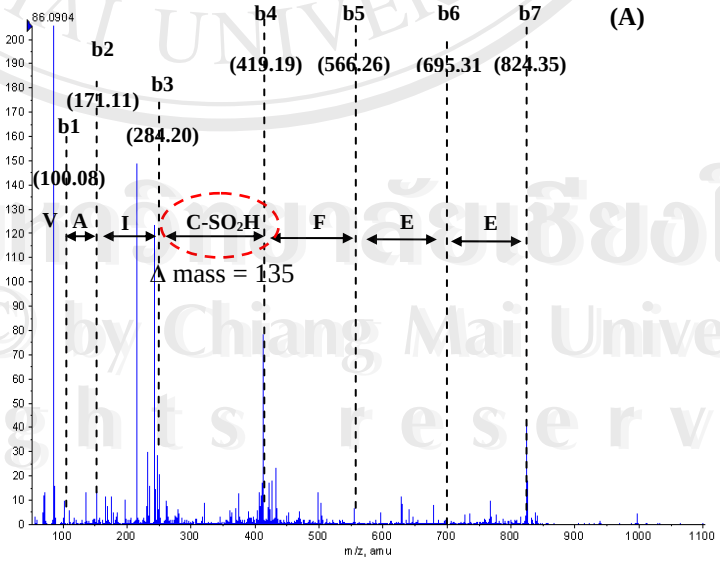

Figure 3.25 Collision-induced disassociation (CID) spectrum of the 598 *m/z* peak from Prx II

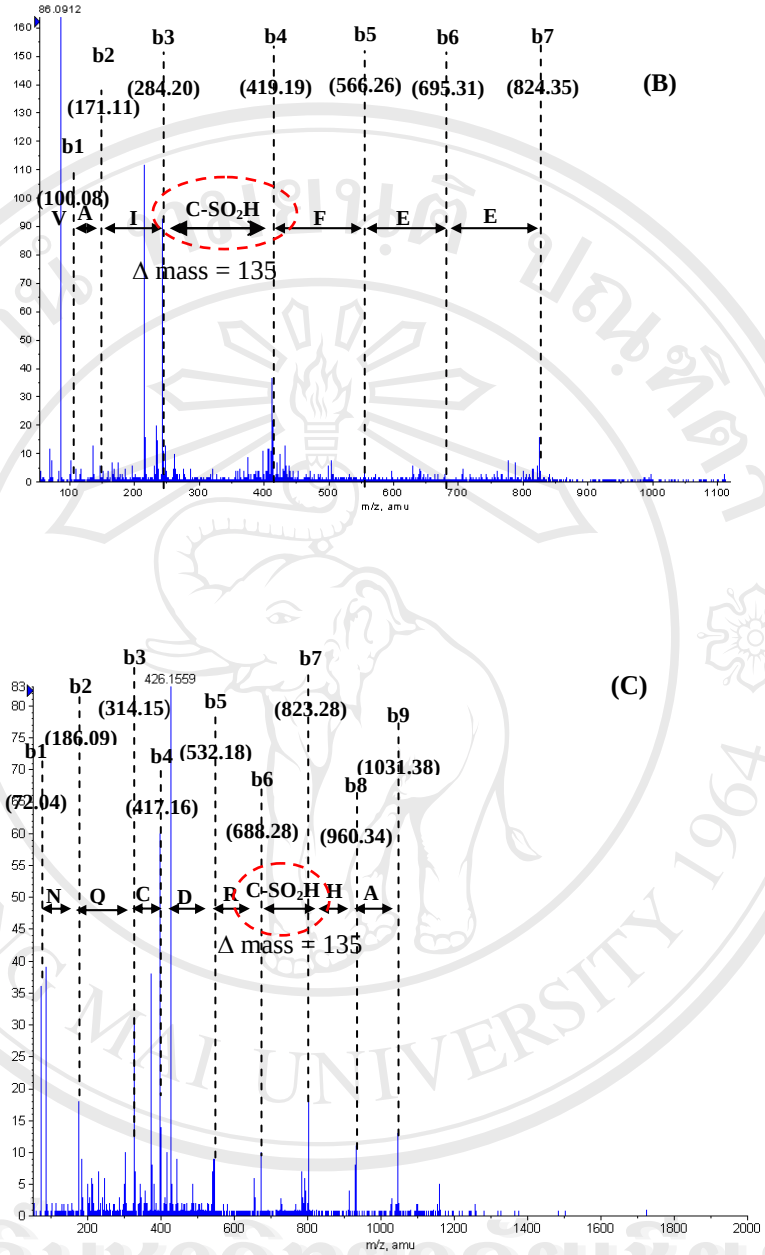

Figure 3.25 (continued) Collision-induced disassociation (CID) spectrum of 598 *m/z* peak (B) and 809 *m/z* peak from Prx III. The amino acid sequences were calculated from the difference of mass units of b ion series. The 135 mass difference was derived from cysteine molecular weight (103) plus two oxygen atom (32).

3.4) USING CY3 MALEIMIDE FOR DETECTION THIOL OXIDIZED PROTEINS IN *BACILLUS STEAROTHERMOPHILUS* TLS33

3.4 Using Cy3 Maleimide to detect thiol oxidative modified proteins.

Cysteine is one of the most rarely used amino acids in the proteins of most organisms studied so far. Therefore, when highly conserved in proteins, it usually plays crucial roles in the structure, function, or regulation of the protein. This is due to the ability of thiol groups to stabilize protein structures by forming covalent disulfide bonds and to coordinate metal ions, as well as due to their high reactivity and redox properties. Proteins in the extracellular space and oxidizing cell compartments. (e.g endoplasmic reticulum and periplasm) often rely on disulfide bonds to support their correct folding. And maintain their structural stability. Cellular defense strategies that are activated in response to increased levels of reactive oxygen species include thiol-containing peroxidases and disulphide reducing enzymes. Furthermore, the activity of several proteins is modulated by a reversible thiol modification, e.g. peroxide-specific regulator OxyR, the zine-coordinating chaperone Hsp33 and the cobalmine-independent methionine synthase MetE of *Eschericia coli* (108) In addition, the generation of the non-reducible thiol derivatives sulfinic acid and sulfonic acid under oxidative stress conditions has also been reported. In *Stapphylococus aureus*, it was demonstrated that treatment with high concentrations of H_2O_2 forces the generation of cysteine sulfonic acid of Cys-151 in glyceraldehydes-3-phosphate dehydrogenase (109).

The Gram-positive model organism *Bacillus subtilis* has been extensively analyzed to characterize the stress physiology after exposure to oxidative. By means of transcriptomics and proteomics, massive changes of gene expression and protein synthesis were observed when *B. subtilis* cells were exposed to superoxide (O_2), H_2O_2. In contrast to the detailed characterization of the gene expression less effort was made to identify the biological targets of reactive oxygen species. A first attempt to globally monitor irreversible protein oxidation in *B. subtilis* revealed a strong increase of protein carbonyl groups in H_2O_2- treated cells (110).

Cy3 Maleimide was applied for detection of thiol oxidized proteins. The Maleimide group is reactive functional group which this fluorescence dye contained. It can specific react to free sulfydryl group or –SH of cysteine residues. The double bond in this functional group will be spontaneous broke up. And the either carbon will be bind to the –SH by covalent bonding resulting in the proteins will be labeled.

In addition, the Cy3 is a fluorescence dye which was used in differential in-gel electrophoresis or 2D-DIGE. Thus, this dye is friendly to Typhoon scanner and Imager FX pro plus. Furthermore, this methodology can be further developed to using DIGE for studying differential oxidative conditions. Otherwise, this dye is more convenient and safe than isotopes thus it could be high benefit of using this dye. The non oxidized free sulfydryl group will be blocked with alkylating agent, iodoacetamide (IAM) in order to prevent labeling on non-oxidized sulfydryl group. Subsequently, the oxidized –SH group which was form sulfinic acid –SOH in the protein will be further reduced back to –SH by Tris-(2-carboxyethyl)-phosphine (TCEP). At this moment, the free sulfydryl group which was from reduction back by

TCEP will be further labeled with Cy3 Maleimide. Thus, eventually we can visualize proteins which were modified with ROS at thiol group of cysteine residue. In this study, the thermophile *B. stearothermophilus* TLS 33 were treated with H_2O_2 which is an strongly oxidant reagent The hydrogen peroxide will generate O_2^-. This molecule will oxidize –SH and it will become –SOH, $-SO_2H$ and $–SO_3H$. The figure 3.26 demonstrated the proteins which were detected by using Cy3 Maleimide labeling. The Image gels were scanned by using wavelength 532 nm with Imager Fx Pro Plus ™.

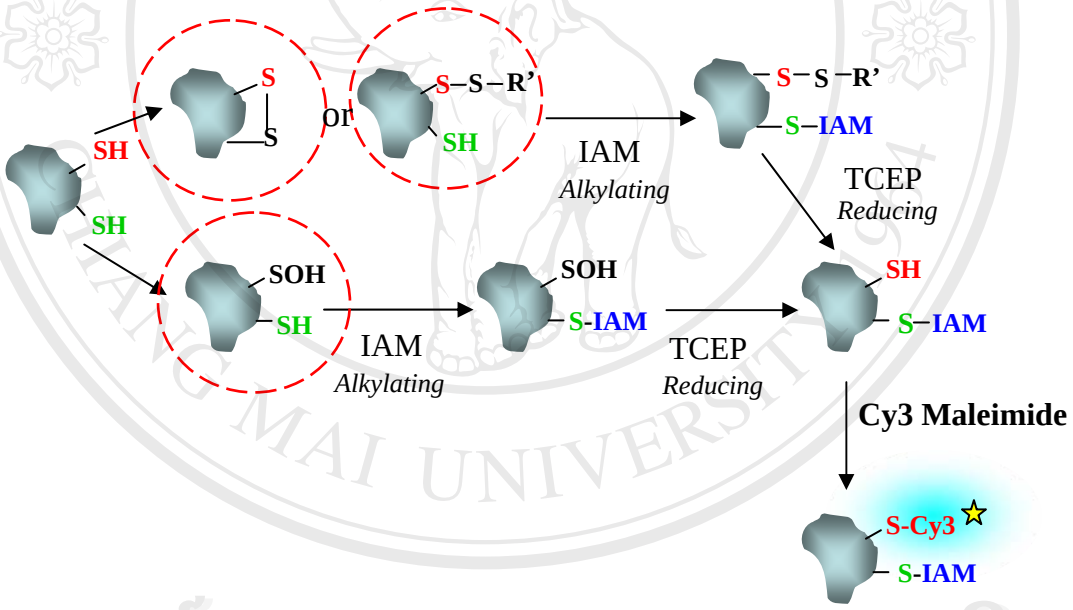

Figure 3.26 The Cy3 Maleimide methodology labeling on thiol oxidized proteins in *B. stearothermophilus* TLS 33.

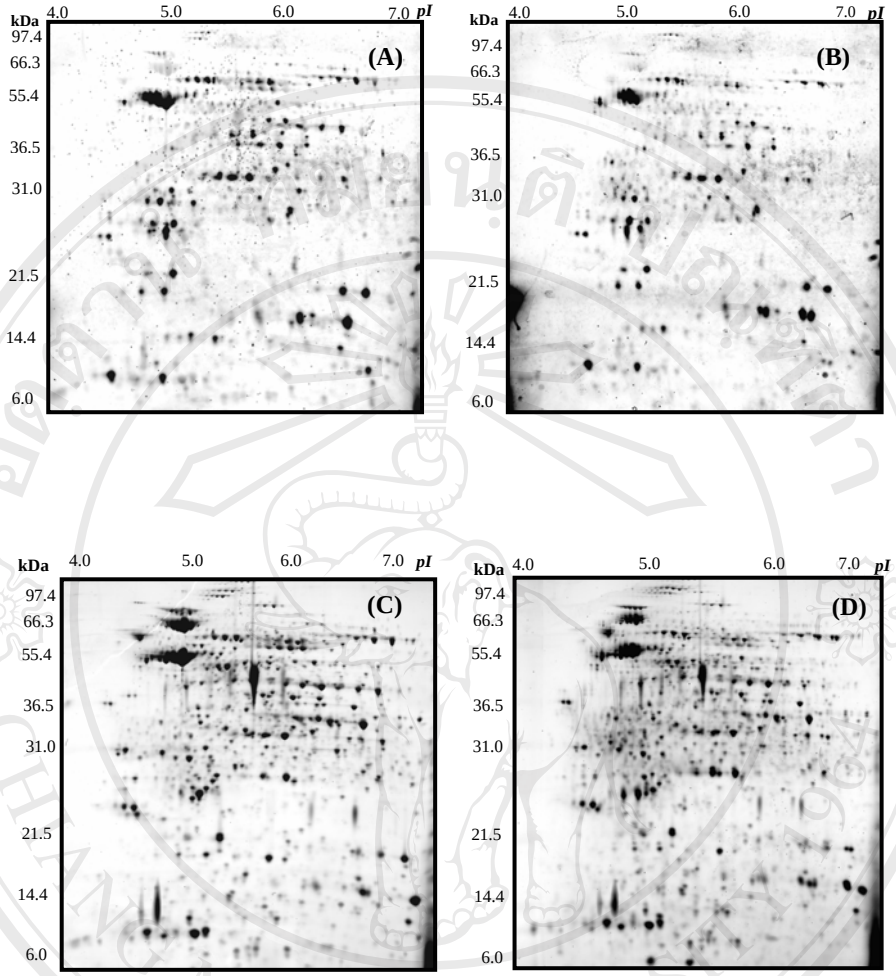

Figure 3.27 2DE image of Cy3 Maleimide labeled on thiol oxidized proteins *B. stearothermophillus* TLS 33 (A) and (B) are the 2DE image of thiol oxidized proteins with labeling with Cy3 Maleimide control and 100 µM of H_2O_2 at the mid-log phase respectively with labeling on oxidized protein with Cy3 Maleimide. And (C) and (D) are 2DE gel stained with Sypro Ruby image of control and 100 µM of H_2O_2 at the mid-log phase respectively.

Each protein spot was identified by MALDI-TOF. The protein identification was performed by using Protein Mass Fingerprint (PMF). The protein reliability was based on P-value of MASCOT software. For protein spot ratio analysis, the image gels were analyzed by PDQUEST software and the identified protein spots as well as their ratio were showed in table 3.4 and figure 3.28 (master gel). The protein functions were classified as cellular function, metabolic pathway as shown in table 3.5.

However, after scanning of Cy3 Maleimide, 2DE gels were post-labeling stained with Sypro Ruby for visualization of total proteins. It was found that several spots were able to be detected by Sypro Ruby staining but they were not able to be visualized by the Cy3 Maleimide methodology. In contrast, a few protein spots were only detected in the Cy3 Maleimide image but were absent in the total protein image (Figure 3.28 C and D). From the results, the spot number in Sypro Ruby staining 2DE gel images are more than Cy3 labeling images. On the other hand, these proteins do not have thiol oxidized –SH or –SOH in their molecules.

Furthermore, this study used Pro Q Diamond which is a reagent for staining phosphoprotein. Due to it was believed that this reagent can detect oxidized proteins or the proteins containing negative charges. Thus it was used for staining proteins from *B. stearothermophilus* TLS33 in both of control sample and treated with H_2O_2 sample. After scanning or image acquisition, they also were post-stained with Sypro Ruby for viewing total protein (Figure 3.30). However, it was further studied the protein expression with image analysis software in the control and treated with H_2O_2 samples. The spot ratio were derived from spot quantities by using protein spot in

control sample as reference ratio or on the other hand, using for dividing spot quantities in treated sample.

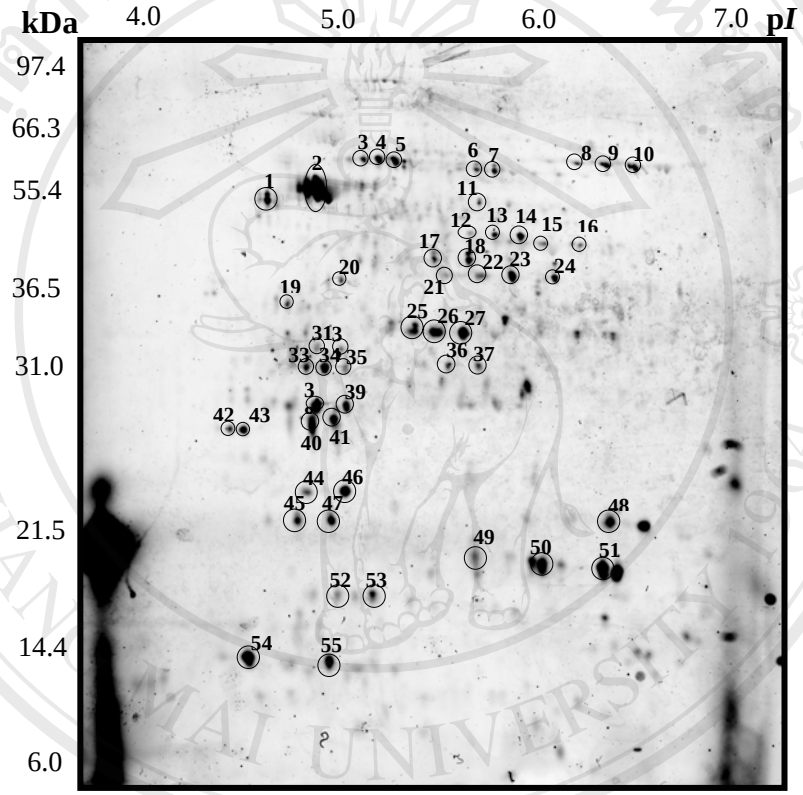

Figure 3.28 2DE image of thiol oxidized proteins which were labeled with Cy3 Maleimide. The proteins were identified and were shown in Table 3.3 for their description.

Table 3.4 The thiol oxidized proteins with labeling with Cy3 Maleimide. These proteins were identified by MALDI-TOF Mass Spectrometry.

spot no.	Protein	Description	Cys	Ratio*
1	EF-TU	Elongation Factor TU	1	2.08
2	GroEL	60 kDa Chaperonin GroEL	1	0.88
3	RimL	Acetyltransferases	4	2.89
4	DnaK	Heat Shock protein DnaK	5	2.03
5	Ilvc	ketol-acid reductoisomerase	3	0.50
6	Spo III EA	spoIIIEA protein	3	0.44
7	Rex	redox-sensing transcriptional repressor	3	0.62
8	SrrB	sensor histidine kinase SrrB, putative	4	4.02
9	FtsZ	ftsZ/tubulin-related protein	4	1.06
10	PyrB	Aspatate carbamolytransferase	3	0.48
11	PutA	NADP-depentdent glyceraldehyde-3-phosphate	1	0.16
12	LDH	L-lactate dehydrogenase	2	0.62
13	LDH	L-lactate dehydrogenase	2	0.65
14	LDH	L-lactate dehydrogenase	2	1.15
15	COG	RNA-binding S4	2	0.39
16	ABC_ATPase	ABC-transporter ATPase	5	0.37
17	PyrB	Aspartate carbamoyltransferase	2	0.08
18	Fmt	Met-tRNAi formyl transferase	1	0.48
19	Pmsr	Peptide methionine sulfoxide reductase	5	3.56

Table 3.4 (continued)

spot no.	Protein	Description	Cys	Ratio*
20	NADH Hydrogeanse	NADH hydrogenase	2	5.65
21	AP2Ec	Endonuclease IV	6	0.00
22	BioA	Adenosylmethionine-8-amino-7-oxononanoate aminotransferase	6	0.72
23	HrcA	Transcriptional repressor of class I heat shock genes	1	1.12
24	ETF-alpha	Electron transferase flavoprotein alpha subunit	4	1.43
25	Fba	Fructose-bisophosphate aldolase	3	0.14
26	Fba	Fructose-bisphosphate aldolase	3	0.69
27	Fba	Fructose-bisphosphate aldolase	3	0.85
28	RSBT	Serine/theronine protein kinase	3	1.20
29	GapDH	Glyceraldehyde-3-phosphate dehydrogenase	1	4.40
30	HMBS	Porphobilinogen deaminase	4	1.44
31	LysR	Transcriptional regulator (LysR family)	1	1.12
32	TPP	Thiamine pyrophosphase	4	0.11
33	Adh_short	Probable oxidoreductase	2	0.51
34	SAICAR	phosphoribosylaminoimidazole - succinocarboxamide synthase	1	0.76
35	ParB	ParB-like partition protein	6	2.14
36	adh_short	Short chain oxidoreductase	2	4.02
37	HisM	ABC-type amino acid transport system, permease component	2	0.63

Table 3.4 (continued)

spot no.	Protein	Description	Cys	Ratio*
38	Sigma-70	RNA polymerase sigma-70 factor, ECF subfamily	2	0.00
39	PP2C	Protein phosphatase 2C-like	4	0.21
40	AhpC	Alkyl hydrogen peroxidase C	3	6.19
41	GntR	Transcriptional regulator	1	0.27
42	PPT	Pyrophosphatase	2	0.00
43	PPT	Pyrophosphatase	2	3.17
44	Tpx	Thiol peroxidase	2	3.60
45	Tpx	Thiol peroxidase	2	3.76
46	Tpx	Thiol peroxidase	2	1.38
47	CTD_DOD	Cytidine-deoxycytidylate deaminase	8	1.11
48	Tpx	Thiol peroxidase	2	1.11
49	Mob	Molybdoptein cofactor biosyntheis protein	4	8.66
50	PPT	Phophotransferase enzyme	5	1.74
51	UspA	Universal stress protein	2	0.97
52	G3P_CTD	Glycerol-3-phosphate cytidyltransferase	5	0.93
53	GlyA	Glycine hydroxymethyltransferase	5	0.00
54	Duf322	Putative stress response protein	2	3.07
55	GroES	10 kDa Chaperonin GroES	1	0.95

**** Ratio was derived from spot intensity in treated sample to spot intensity in control***

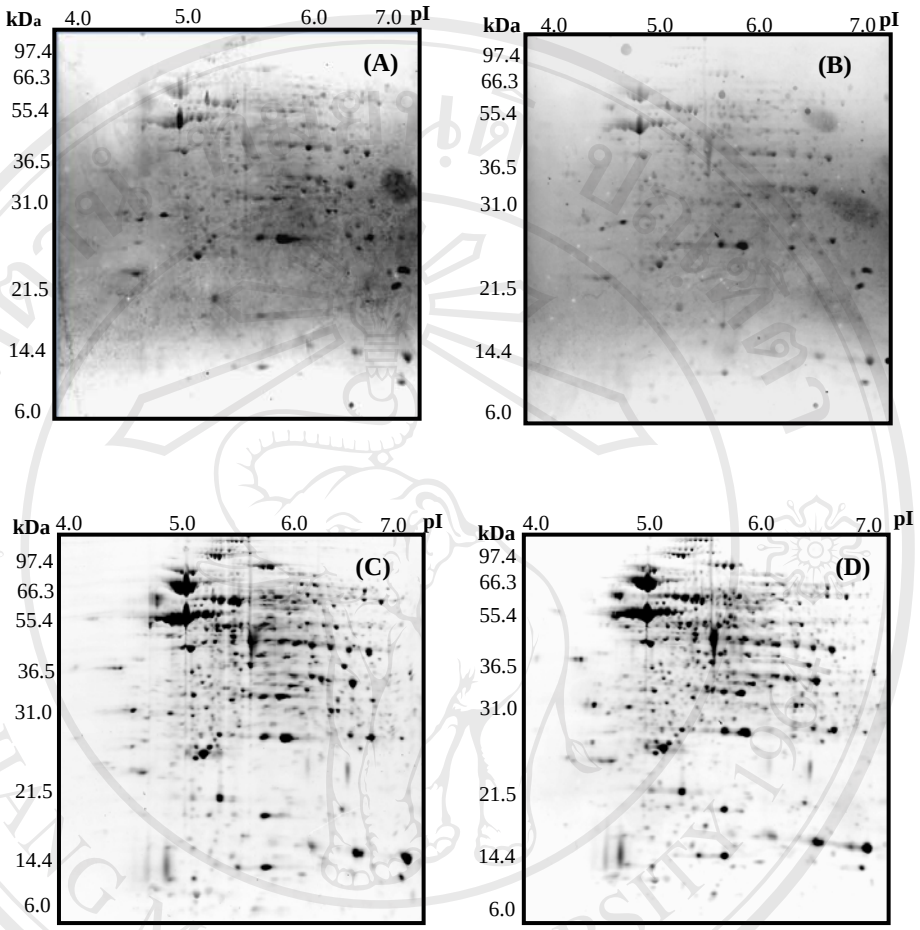

Figure 3.29 2DE gel of Pro Q Diamond staining of intracellular proteins of *Bacillus stearothermophilus* TLS33. (A) and (B) are gels stained with ProQ Diamond control and treat with 100 µM of H_2O_2 , respectively. (C) and (D) are gel post-stained with Sypro Ruby for viewing total proteins in control and 100 µM of H_2O_2 respectively.

According to protein staining, Pro Q Diamond, phosphoprotein staining. This reagent was applied in several works (111,112). In this study, it was used for investigation proteins which were believed that it is able to detect oxidized proteins due to it can detect phosphoproteins which containing phosphate group (PO_4^-) or negative charge. Nevertheless, it was found that this staining was not corresponding to Cy3 Maleimide labeling methodology (Figure 3.27 and 3.29) which a number of protein spots were visualized in Pro Q staining image but they were unable to visualize in Cy3 Maleimide labeling methodology image. In the contrast, some proteins were unable to be visualized with ProQ Diamond staining but they could visualize in Cy3 Maleimide. Therefore, it could indicate that ProQ Diamond was unable staining thiol oxidative modified proteins. This could be suggested that Pro Q Diamond staining might be only able to visualize phosphate groups in protein. Likewise, Cy3 Maleimide labeling methodology could visualize only thiol oxidized proteins. Also, the figure 3.30 demonstrated that there were several proteins can be visualized in the gel images when Cy3 Maleimide methodology was performed by means of no blocking free sulfydryl group with iodoacetamide (IAM). In addition, the numbers of protein spots of no blocking-with IAM gel images are markedly more than free sulfydryl group-blocking image gel (Figure 3.27). Therefore, it could suggest that this Cy3 Maleimide is able to specific visualize thiol modified proteins. However, the Cy3 Maleimide no blocking image gels are very similarly to total protein image gel or Sypro Ruby staining gel (Figure 3.27). This could suggest that Cy3 Maleimide can label on many proteins when there was no blocking. Subsequently, the thiol oxidized protein spots in figure 3.27 were excised from the

gels and characterized by MALDI-TOF mass fingerprint are in table 3.4 and figure 3.28 which has mentioned above.

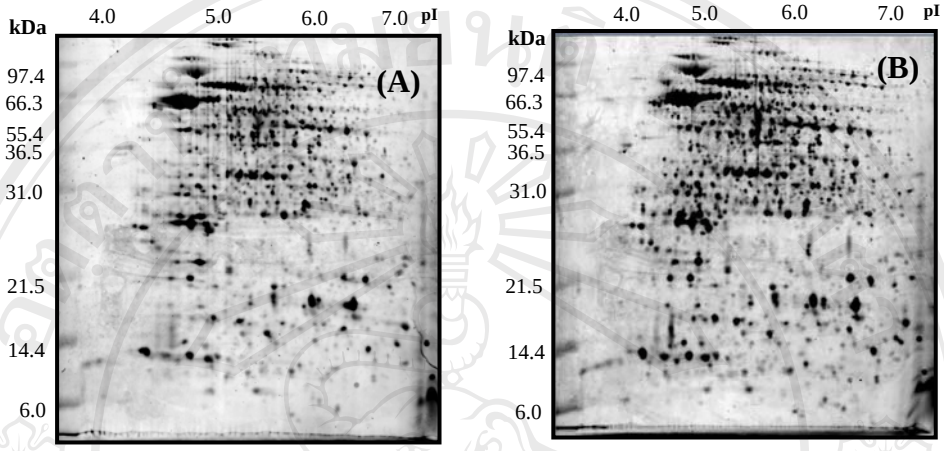

Figure 3.30 The gel images of Cy3 Maleimide labeling on the intracellular protein sample with no blocking with IAM before labeling. (A) Control (B) 100 µM H_2O_2 treated

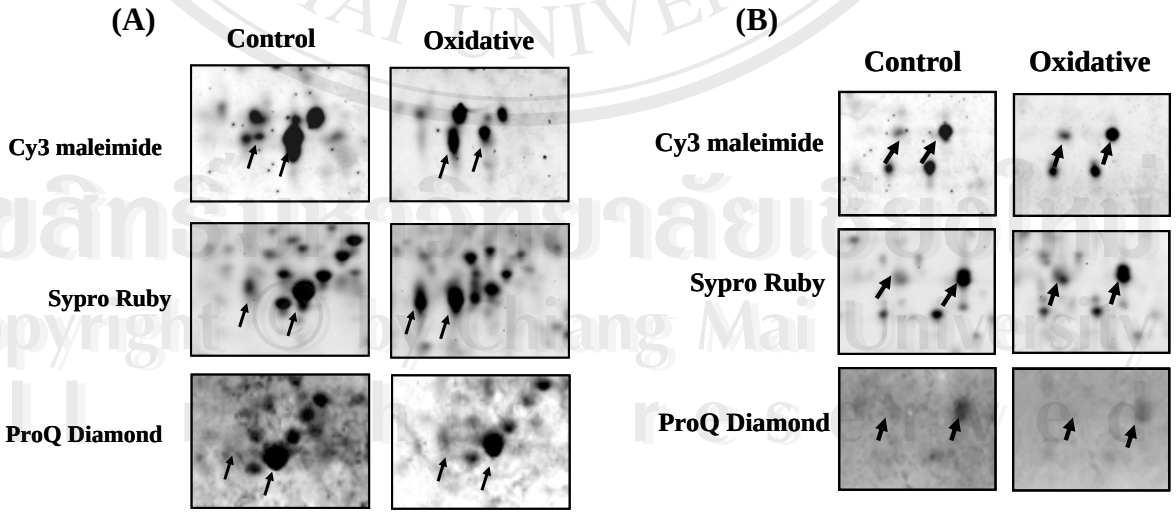

Figure 3.31 The protein spots which were visualized by Cy3 Maleimide methodology. In which, (A) AhpC or Prx protein (B) Tpx

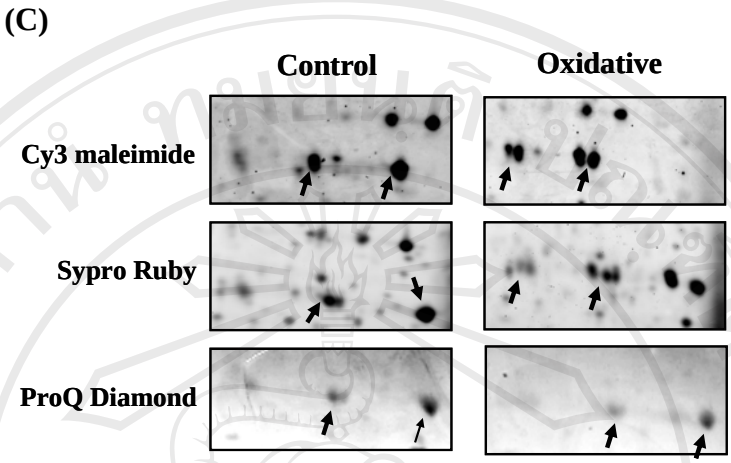

Figure 3.31 (continued) (C) Universal stress protein

3.4.2 Protein identification and protein function classification

After separating protein complex with 2DE, image acquisition and analysis, the interesting protein spots were excised and characterized by means of mass spectrometry. The interesting protein spots were digested with sequencing grade trypsin. The mass peptide fingerprint (PMF) was used for searching of protein identification in the database. MASCOT program from matrixscience was applied for this. In addition, the 55 spots that were detected by Cy3 Maleimide labeling methodology were further identified and were shown in table 3.4. From database searching, it can investigate the cysteine residues in the protein sequence. This could indicate that cysteine plays important biological role in protein. From analysis protein spot quantity with PDQUEST 2-D analysis software, the image gels were normalized in order to set each image gel with same background and this could provide the

accuracy of image analysis. Consequently, the spot ratios were derived. The spot ratios indicated the protein expressions or the protein abundances within the cell. The spot volumes of visualized proteins not only depended on the number of cysteine in protein molecule but also protein abundances in the gels. Form the table 3.5, there were some spots in the gels that has been identified as same proteins, for instance, L-lactate dehydrogenase, fructose-bisphosphate aldolase, alkyl hydrogenperoxidase C, thiol peroxidase etc.

Furthermore, the protein function were classified according to SubtiList database (http://genolist.psteur.fr/subtilist). The function classification are RNA synthesis and transcription regulation, metabolism of carbohydrate and related compounds, metabolism of amino acid and related molecule, metabolism of phosphate, metabolism of lipid, signal transduction and molecular transportation, metabolism of cofactor, unknown function, energy metabolism and detoxification. In this experiment, the major proteins which were able to be detected by Cy3 Maleimide Methodology related to RNA synthesis or transcription or regulation of proteins. In addition, metabolism of carbohydrate and detoxification were the second of protein function which this method can detect (Figure 3.32). Furthermore, for proteins this involved in glycolytic pathway (Figure 3.33). This figure described the generation of NADPH which is molecule that is involved in against oxidant molecule in the cell. Thus, there are many reports concluded that when the cells encounter the oxidative stress, they would express proteins in glycolytic pathway (108-111). Thus, this study has been corresponding to the previous studies. In the figure 3.33, L-lactate dehydrogenase, fructose-bis-phosphate aldolase (Fba), glycerol-3-phosphate dehydrogenase (GADPH) and acetaldehyde dehydrogenase (ADH) involving in

pentose phosphate pathway have been observed that they were up-regulated in Cy3 Maleimide image gel while these proteins also were able to produce NADPH which is reducing co-enzyme. Therefore, it was hypothesized that it can scavenger ROS molecule in the cell (115).

However, there were other protein functions which were observed in this study, for instance, detoxification. AhpC is an enzyme which the bacteria use for scavenger ROS in the cell (117). This enzyme contains reactive cysteine residue in its molecule so that the ROS would react to –SH of cysteine residue in this enzyme. Therefore, this enzyme was detected by Cy3 Methodology. Likewise, thiol peroxidase, this protein is also an oxidant enzyme which involved in anti-oxidant system that could observe by this method as well.

3.4.3 Protein in detoxification

From protein identification and protein function classification, detoxification proteins were also observed. AhpC and Tpx protein were mentioned above. Interestingly, these proteins were shift to acidic region in 2DE gel (Figure 3.31). A few of studies reported that these proteins can react with H_2O_2 and provide sulfenic acid in cysteine residue (38-40). AhpC or Prx could be observed in 3 forms from basic region to acidic region (3 spots). Cy3 Maleimide methodology can visualize only two forms that are original form and second oxidized form (Figure 3.31A). Unlike, Sypro Ruby staining, all three forms could be visualized. For Pro Q diamond, it could be visualize only original form. The visualization of Tpx was similarly to AhpC (Figure 3.31B). Tpx is a protein which involved in anti-oxidization or detoxification in the cell. Likewise,

AhpC, oxidized form of Tpx was visualized in both of oxidized and original form in Cy3 Maleimide methodology. Also, it was visualized in Sypro Ruby staining. Moreover, it was able to be visualized by Pro Q Diamond staining. Both of Tpx and AhpC are proteins involved in anti-oxidative pathway. Therefore, it was assumed that the oxidized thiol group of these proteins might be important to their function. Thus, they can be detected by Cy3 Maleimide method.

For universal stress protein (Figure 3.31C), its function is still unknown currently. However, the previous study suggested that it would be expressed when organisms have been under stress conditions (118). In this study, it was found that this protein was visualized by Cy3 Maleimide, Sypro Ruby including Pro Q Diamond. Universal stress protein was observed that it had three isoforms. In oxidative stress, it has been found that each spot seemed to be shift to acidic region in 2DE gel. This was observed in both of Cy3 Maleimide and Sypro Ruby staining image. In addition, the oxidized form could not be visualized by ProQ Diamond. And the original from of Usp could not be seen in Cy3 image when it was in oxidative stress. Unlike, Sypro Ruby staining is able to visualize all of three isoforms. In summary, Cy3 Maleimide methodology is able to visualize thiol oxidized proteins. And each protein visualization method, Pro Q Diamond, Sypro Ruby Cy3 Maleimide, can detect different protein isoform. In this study, it focused on thiol oxidized proteins which was believed that they have potential to be signaling protein.

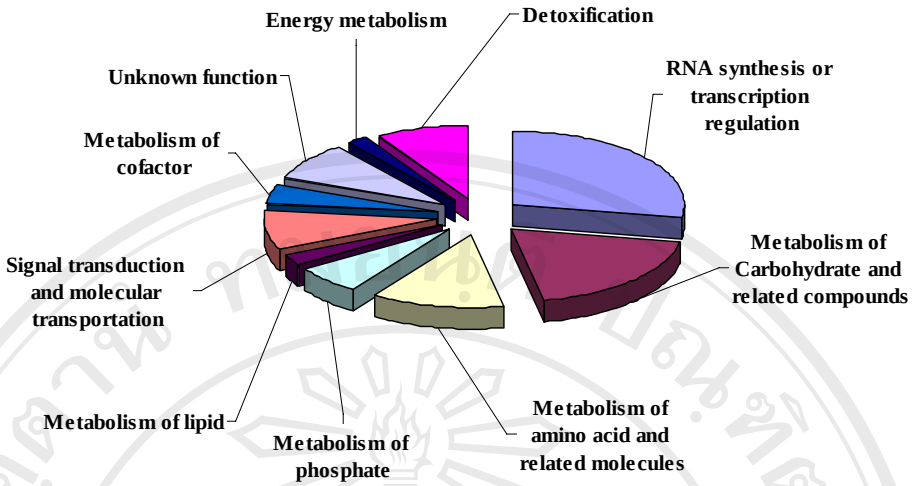

Figure 3.32 Histogram demonstrated proportion of function classification of oxidized proteins in *B. stearothermophilus* TLS33

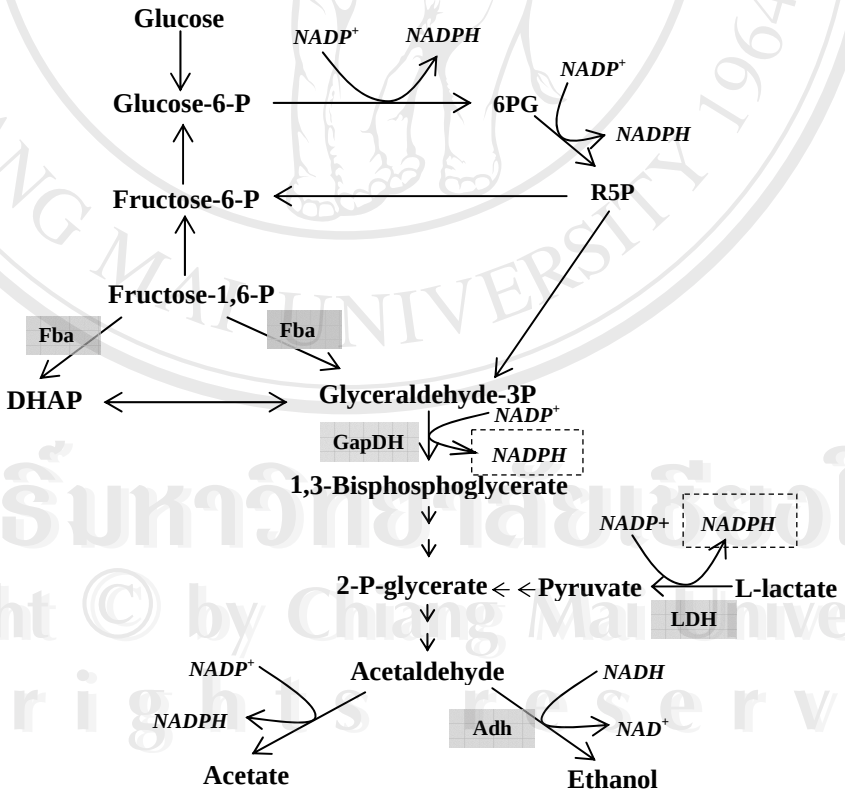

Figure 3.33 Pentose phosphate pathways of the up-regulated proteins found in 2DE-gels were shaded

Table 3.5 Function classification of thiol oxidized proteins in *B. stearotherothermophilus* TLS33

No.	Protein function classification
	RNA synthesis or transcription regulation
1	Elongation factor
2	60 kDa Chaperoin GroEL
3	Heat Shock protein DnaK
4	Spo III EA protein
5	Redox-sensing transcriptional repressor
6	RNA-binding S4
7	Met-RNAi formyl transferase
8	Endonuclease IV
9	Transcriptional repressor of class I heat shock genes
10	Transcriptional regulator (LysR familly)
11	RNA polymerase sigma-70 factor, ECF subfamilly
12	Transcription regulator GntR
13	10 kDa Chaperonin GroES
	Signal transduction and molecular transportation
1	Sensor histidine kinase SrrB, putative
2	ABC-transporter ATPase
3	Serine/threonie protein kinase
4	ABC-type amino acid transport system, permease component

Table 3.5(continued)

No.	Protein function classification
	Metabolism of amino acid and related molecules
1	Ketol-acid reductoisomerase
2	Aspartate carbmolytransferase
3	Adenosylmethionine-8-amino-7-oxonanoate aminotransferase
4	Prophobilinogen deaminase
5	Cytidine-deoxycytidylate deaminase
6	Glycine hydroxymethyltransferase
	Unknown function
1	ftz/tubulin-related protein
2	ParB-like partition protein
3	Universal stress protein
4	Putative stress response protein
	Metabolism of lipid
1	Acetyltransferase
	Metabolism of cofactor
1	Thiamine pyrophosphatase
2	Molybdoptein cofactor biosynthesis protein
	Metabolism of phosphate
1	Phosphotransferase enzyme
2	Protein phosphatase 2C-like
3	Pyrophosphatase

Table 3.5 (continued)

No.	Protein function classification
	Energy metabolism
	Electron transferase flavoprotein alpha subunit
	Metabolism of Carbohydrate and related compounds
1	NADP-dependent glyceraldehyde-3-phosphatase
2	L-lactate dehydrogenase
3	NADH hydrogenase
4	Fructose-bisphosphate aldolase
5	Probable oxidoreductase
6	Acetaldehyde dehydrogenase
7	Pyrophosphatase
8	Glycerol-3-phosphate cytidyltransferase
9	Glyceraldehyde-3-phosphate dehydrogenase
	Detoxification
1	Peptide methionine sulfoxide reductase
2	NADH hydrogenase
3	Alkyl hydrogen peroxidase C
4	Thiol peroxidase

3.5) TWO DIMENSIONAL DIFFERENTIAL IN-GEL ELECTROPHORESIS (2D-DIGE) OF THIOL OXIDIZED PROTEINS

The differential In-gel Electrophoresis (DIGE) technique is aimed at improving reproducibility. To analyze the samples in DIGE, two spots of proteins extracts are labeled proteins are mixed and separated in the same 2DE gel. The 2D-gel patterns can be rapidly imaged by the fluorescence excitation of either Cy3 or Cy5 dyes. The amount of the dye is controlled in such a way that on average one protein molecule is labeled not more than once and minimum number of molecules of each protein is labeled. A comparison of the resulting images allows quantitation of each protein spot. Since two pools of the proteins are separated the same gels, those proteins existing in both pools will migrate to the same locations in 2DE gel, minimizing the reproducibility problem. Quantitaion of the protein profile can be rapidly and accurately achieved based on the fluorescence intensity. Thus, the DIGE technology has adequate sensitivity, reproducibility and wide dynamic range. But this study attempted to modify DIGE method because of its sensitivity and reproducibility for detection of thiol oxidized proteins. Normally, the proteins will be labeled with Cydye (Cy3 and Cy5) which have N-hydroxy-succinimide ester as the functional group labeling on ε-NH_2 of Lysine residue of the proteins. But this study applied another CyDye containing Maleimide as functional group. Because of Maleimide is able to specific covalently bind to –SH of proteins, so it was applied for labeling thiol oxidized proteins. The figure 3.34 demonstrated the CyDye labeling on thiol oxidized proteins methodology. The free –SH of proteins was blocked with alkylating agent, iodoacetamide (IAM) and subsequently, the oxidized –SH was reduced by tris-(2-

carboxyethyl)-phosphine (TCEP). Finally the CyDye Maleimide is able to label the nascent reduced –SH.

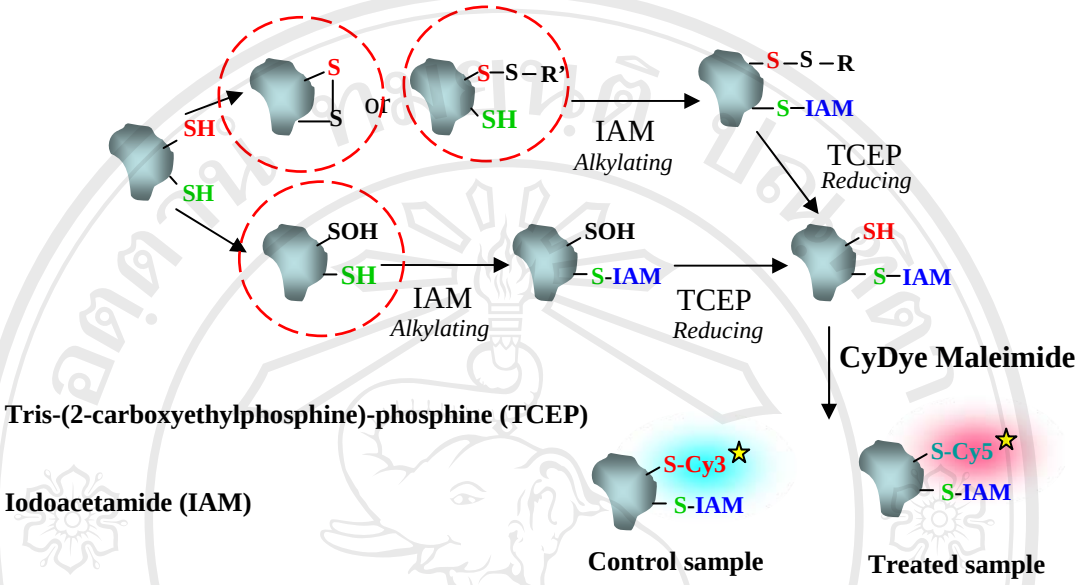

Figure 3.34 The DIGE technique for detection of thiol oxidized proteins

In this study, the proteins of control sample were labeled with Cy3 Maleimide and treated sample were labeled with Cy5 Maleimide. After that the proteins in each sample was pooled together and performed in the same 2DE gel. Cy3 is excited at 540 nm and has an emission maximum at 590 nm, while Cy5 is excited at 620 nm and emits at 680 nm. Thus, the 2DE gel was scanner with different wavelengths for generation different images. The Cy3 image was set as green color while Cy5 image was set as red color. The 2DE image analysis was able to combine two images into the same image gel (Figure 3.35). Thus the spots in the same location as another gel image became to yellow color because when the red color was combined with green color, it will become yellow, which has demonstrated in figure 3.35.

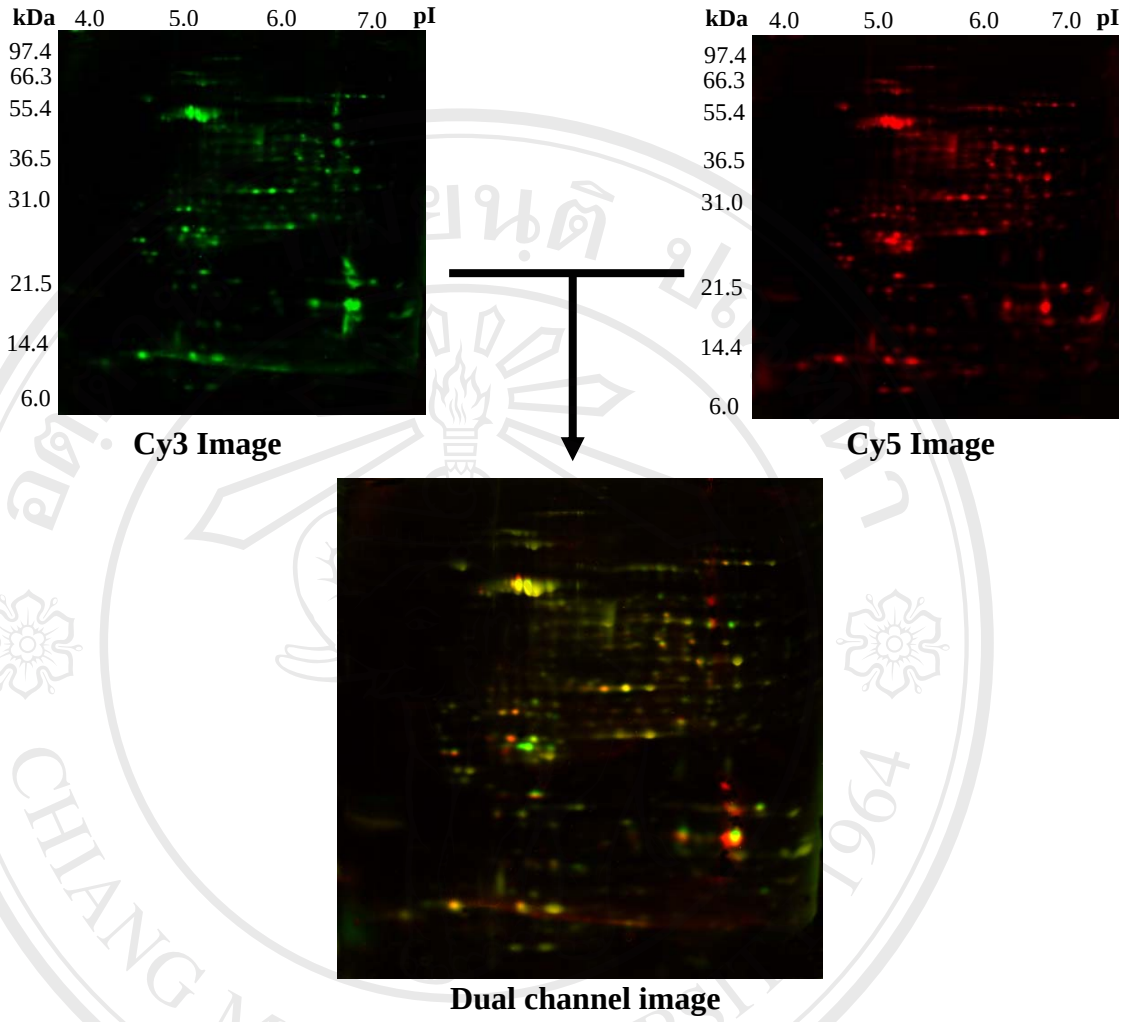

Figure 3.35 The 2D-DIGE image of 100 µM H_2O_2 treated *B. stearothermophilus* TLS33

In this study, the *B. stearothermophilus* TLS33 was treated with 50 M and 100 M of H_2O_2 and its proteins were labeled with CyDye which the method has been demonstrated in figure 3.4. The figure 3.35 showed the 2D-DIGE image of 50 µM and 100 µM H_2O_2 treated samples of *B. stearothermomphilus* TLS33

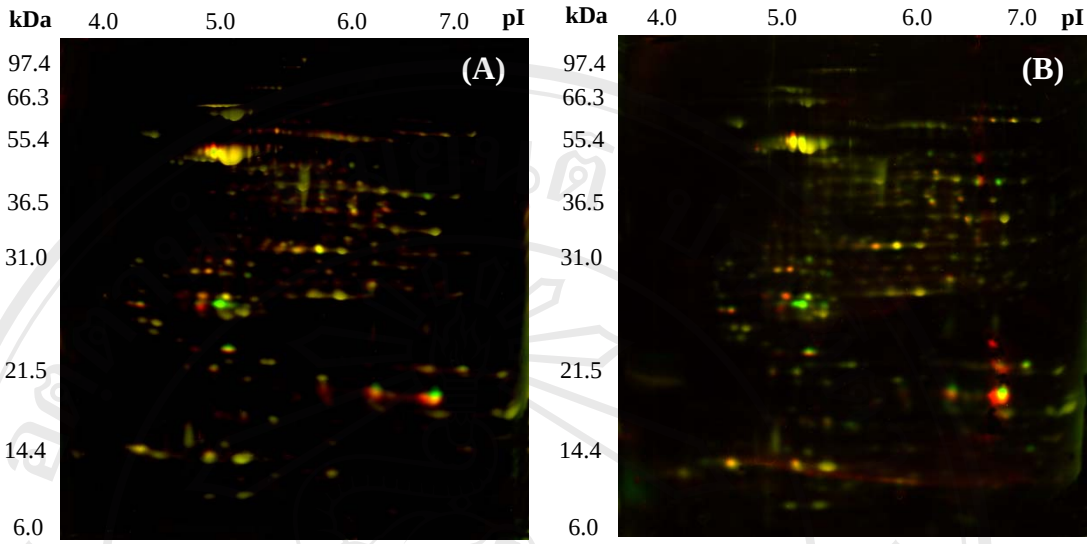

Figure 3.36 2D-DIGE gel images of the *B. stearothermophilus* TLS33 proteins after treated with 50 µM H_2O_2 (A) and 100 µM H_2O_2 (B) for 15 minutes

After the scanning of 2D-DIGE gels, the 2D-DIGE gel images were analyzed by PDQUEST 2-D analysis software and generated dual channel images (combined images of Cy3 image and Cy5 image) which have been showed in figure 3.36. From the results, it could be found that there were a number of protein spots that were differentially expressed which indicating those proteins containing thiol oxidized group. The figure 3.37 demonstrated the selected proteins involving pentose phosphate pathway. The protein ratio was derived from the spot intensity from Cy5 image (red, treated sample) to the spot intensity from Cy3 image (green, control sample). In addition, the color stripe was generated for investigation of changes of green color to red color of protein spots corresponding the protein ratio. Nevertheless, these proteins contained Cysteines.

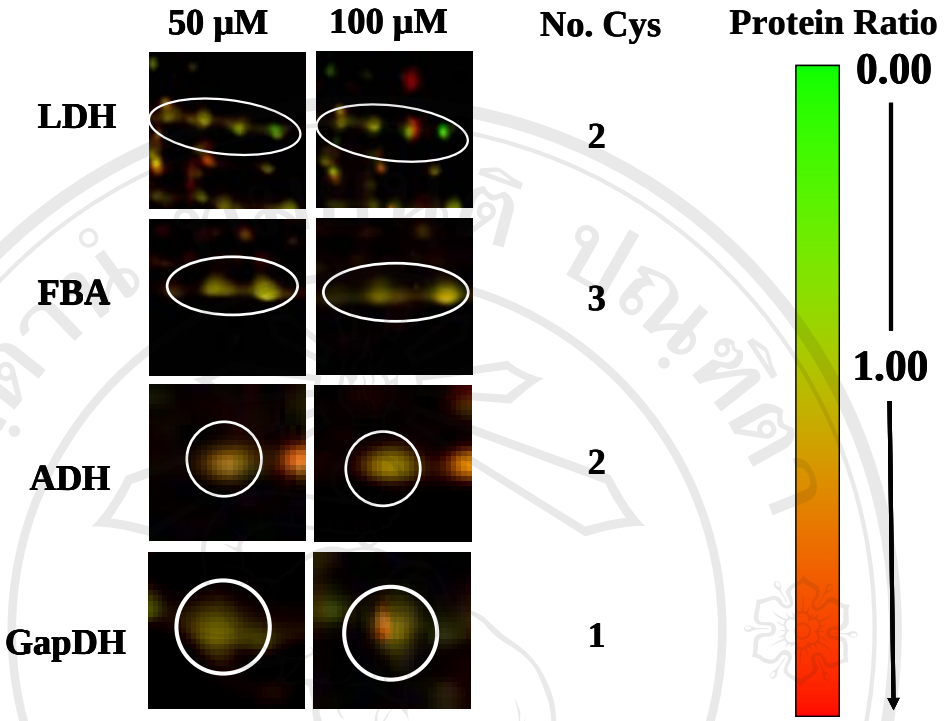

Figure 3.37 The differentially expressed proteins in 2D-DIGE image involving in pentose phosphate pathway. 50 µM and 100 µM are the concentration of H_2O_2 which treated *B. stearothermophilus* TLS33.

From the results in figure 3.37, L-lactate dehydrogenase (LDH) seemed to be shift to more acidic region which is similar to Prx that has been mentioned in the previous topics. In generally, LDH is a protein in pentose phosphate pathway, but this result indicated that this protein was oxidized so it could be visualized by DIGE labeling methodology. In addition, it seemed that it had four isoforms and an isoform was shift when this bacterium was treated with 50 µM and 100 µM H_2O_2. So, it was observed in green color that meant a LDH isoform was presence under non oxidative stress

while the yellow spots of LDH indicated there were these isoforms in both of absent of H_2O_2 and oxidative conditions. Acetaldehyde dehydrogenase was slightly up-regulated, therefore, the orange color was obtained (see the color stripe and protein ratio). Likewise, glyceral-3-aldehyde dehydrogenase, GADPH, its spots were orange as well. Whereas fructose-3-biphosphate dehydrogenase (FBH) spots were yellow color that meant their abundances in control and oxidative were not much changed. The figure 3.38 demonstrated the proteins involving redox metabolism pathway.

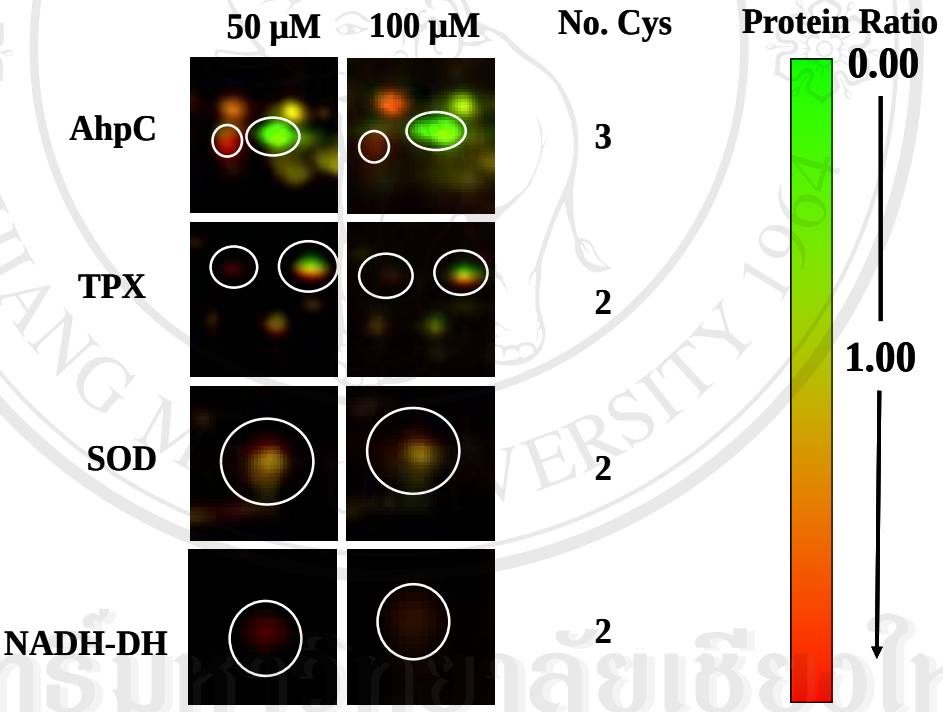

Figure 3.38 The differentially expressed proteins in 2D-DIGE image involving in redox metabolism. 50 µM and 100 µM are the concentration of H_2O_2 which treated *B. stearothermophilus* TLS33.

From the result in figure 3.38, alkyl hydrogenperoxidase C (AhpC) abundance in H_2O absent condition (green) seemed to be markedly more than in the oxidative stresses. Similar to thiol peroxidase (TPX), its abundance was higher than in oxidative stress. When the bacterium was under the oxidative stress, the results have indicated that the red spots these proteins were appeared. That could indicate that these proteins shift to the acidic region in 2DE gel. However, they were slightly appeared, unlike in control condition. Due to they act as H_2O_2 scavenger enzyme that has been mentioned in the previous topics. Therefore, they would shift to more acidic region. Interestingly, NADH dehydrogenase (NADH DH) was expressed while the bacterium was treated with 50 µM and 100 µM of H_2O_2. Therefore, the red spot of NADH DH was observed. Furthermore, there was no the green spot of this protein that meant it was expressed in oxidative stress. In addition, superoxide dismutase (SOD) seemed to be slightly up-regulated as well because it was observed that it is orange spots (red > green). The figure 3.39 demonstrated proteins relating to chaperone. In basically, chaperones have many functions and have many kinds. GroEL and GroES act as chaperonin participating in protein folding. The nascent polypeptides must to enter into their cavity and they aid that protein appropriate folding. From the results in figure 3.39, it was found that both of GroEL and GroES was very slightly up-regulated, almost not changes. DnaK is a protein working with GroEL including to HrcA. They are the proteins related to heat shock operon. Interestingly, DnaK was absent when the bacterium was under 100 µM H_2O_2 condition and its spot in 100 µM H_2O_2 was green. Unlike, GroES seemed to be slightly up-regulated. There was also found that HrcA is not changed during oxidative stress.

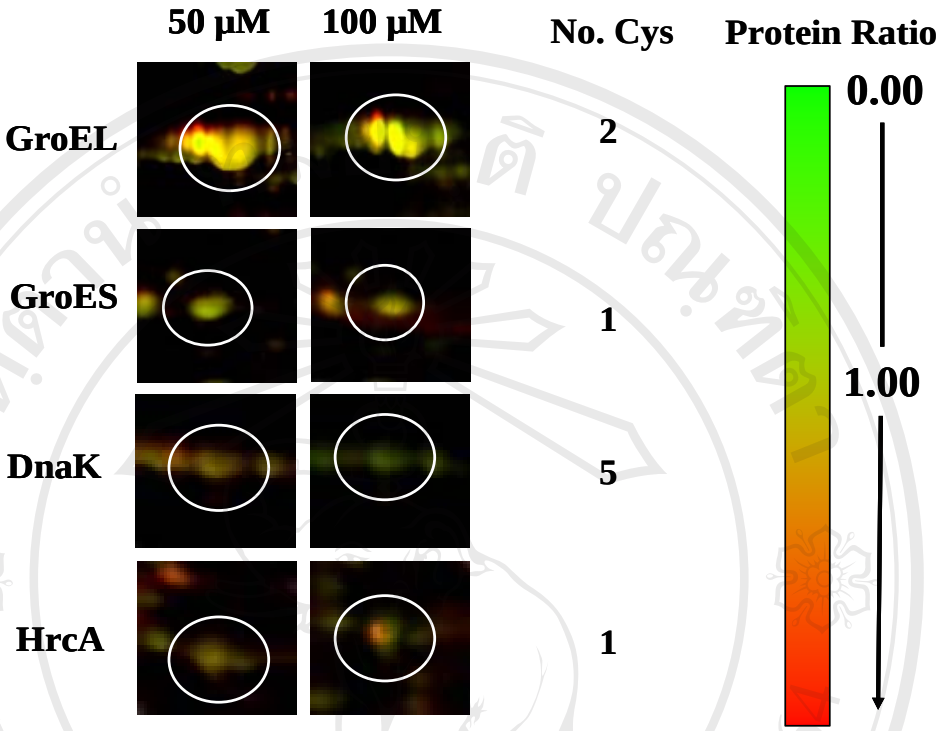

Figure 3.39 The differentially expressed proteins in 2D-DIGE image relating to chaperone. 50 µM and 100 µM are the concentration of H_2O_2 which treated *B. stearothermophilus* TLS33.

In summary, the DIGE methodology could be a method that was able to detection of thiol oxidized proteins which have the potential to be signaling proteins or related to other metabolisms within the organism cell. Due to it has been applied two different dyes, Cy3 and Cy5, which have different emission wavelengths. The reproducibility and sensitivity could be obtained in this study.